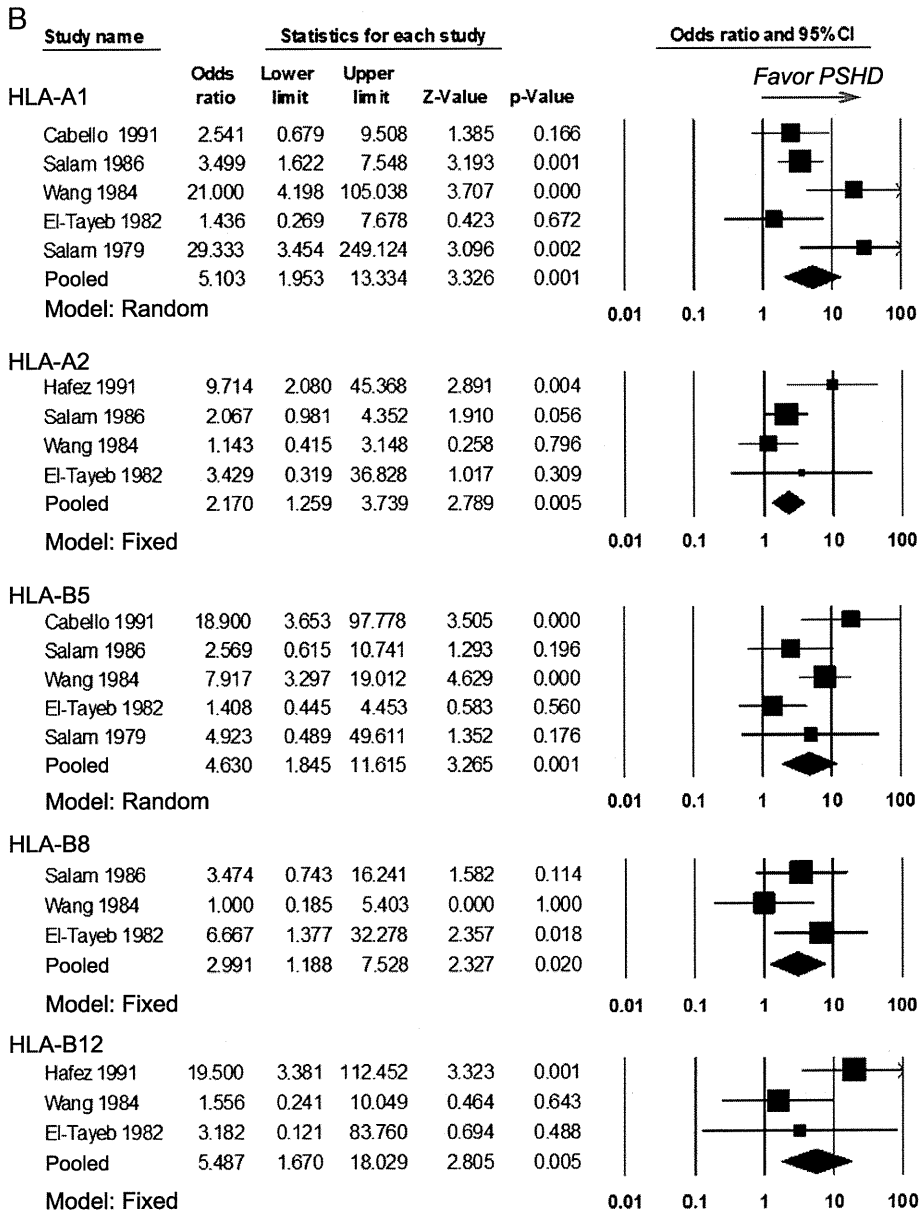

Fig. 2 (*continued*).

conflicting effects. Moreover, other hepatitis diseases, alcohol intake, smoking, and praziquantel treatment doses can all affect the development of PSHD [2], and therefore may have affected our analysis. However, because meta-analyses use selected studies based on defined criteria, they can assess common and significant genetic factors that were not assessed in a systematic way in individual, primary studies. Similar meta-analyses of the genetic studies of pneumococcal and meningococcal infection [71], autoimmune diseases [72,73], and cancer [74] have been already reported. We found no effect of different schistosomal species on the outcome of PSHD; however, the number of studies for each allele was small (less than 5), and further studies should focus on this issue.

In conclusion, the association between post-schistosomal hepatic disorder and risk factors including eggs load, lack of treatment, repeated infection and HLA types has been reported in previous studies. However, to the knowledge of the authors this is the first systemic meta-analysis that combines individual studies to improve the strength of the evidence. This meta-analysis identified positive associations between eight HLA types – DQB1*0201, DQB1*0303, DRB1*0901, A1, A2, B5, B8, and B12 – and post-schistosomal hepatic disorder and negative associations with two variants, DQA1*0501 and DQB1*0301. Moreover, we identified the possible existence of common antigenic moieties that would be presented to some pathogenic or protective T-cells that could affect the outcome of the disease. Though previous included studies identified a positive association of DRB1*0901-DQB1*0303 linkage [41] and negative association of DQA1*0501-DQB1*0301 haplotype [42] with PSHD, we further propose that individuals bearing the DRB1*0901-DQB1*0201 and A1-B8 haplotypes may be at increased risk for the development of PSHD, but further studies are required to confirm our hypothesis.

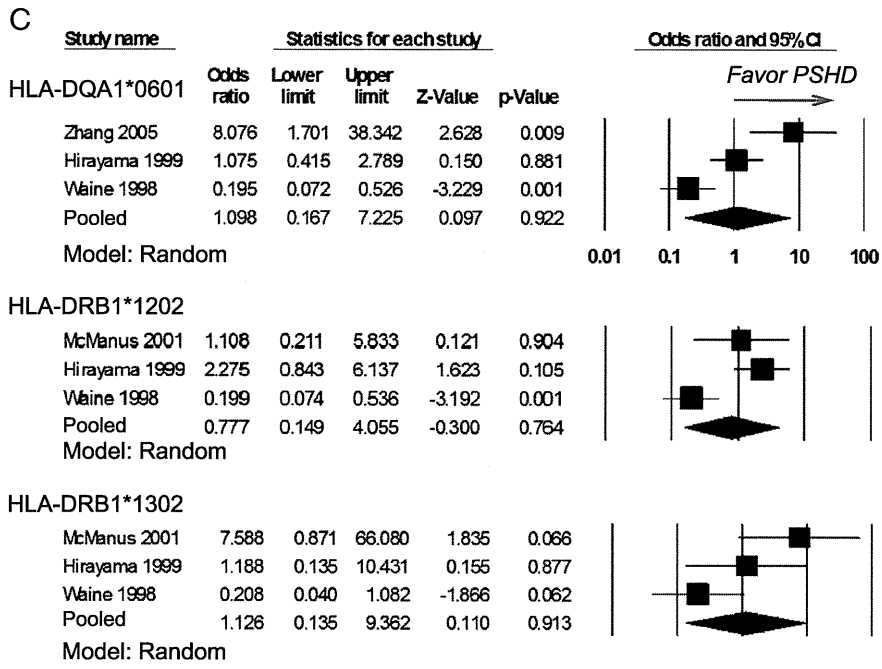

Fig. 2 (*continued*).

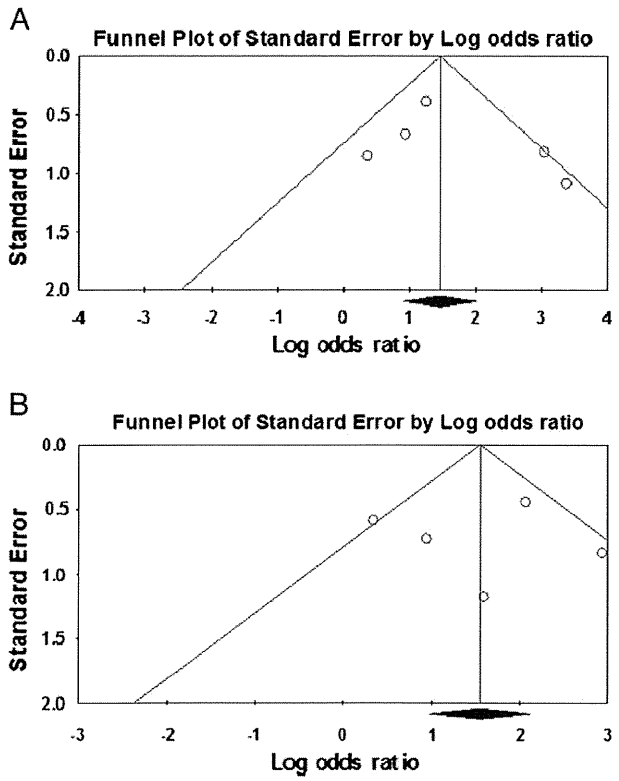

Fig. 3. Funnel plots for evaluation of publication bias of HLA-A1 (A) and HLA-B5 (B) where there are at least five studies on the same genetic variation. Each circle represents each study in the meta-analysis.

Acknowledgments

This work was also supported in part by a Grand-in-Aid for Young Scientists (17301870, 2008–2010 for NTH) from the Ministry of Education, Culture, Sports, Science and Technology (MEXT, Japan), and was supported in part by a Grant-in-Aid for Scientific Research from Nagasaki University to NTH (2007–2009). This study was also supported in part by the Global COE Program (2008–2012) and Japan Initiative for Global Research Network on Infectious Diseases (J-GRID) for KH.

References

[1] van der Werf MJ, de Vlas SJ, Brooker S, Looman CW, Nagelkerke NJ, Habbema JD, et al. Quantification of clinical morbidity associated with schistosome infection in sub-Saharan Africa. Acta Trop 2003;86(2–3):125–39.
[2] Ross AG, Bartley PB, Sleigh AC, Olds GR, Li Y, Williams GM, et al. Schistosomiasis. N Engl J Med 2002;346(16):1212–20.
[3] Steinmann P, Keiser J, Bos R, Tanner M, Utzinger J. Schistosomiasis and water resources development: systematic review, meta-analysis, and estimates of people at risk. Lancet Infect Dis 2006;6(7):411–25.
[4] King CH, Dickman K, Tisch DJ. Reassessment of the cost of chronic helmintic infection: a meta-analysis of disability-related outcomes in endemic schistosomiasis. Lancet 2005;365(9470):1561–9.
[5] Gryseels B, Polman K, Clerinx J, Kestens L. Human schistosomiasis. Lancet 2006;368(9541):1106–18.
[6] Doenhoff MJ, Pica-Mattoccia L. Praziquantel for the treatment of schistosomiasis: its use for control in areas with endemic disease and prospects for drug resistance. Expert Rev Anti Infect Ther 2006;4(2):199–210.
[7] Caldas IR, Campi-Azevedo AC, Oliveira LF, Silveira AM, Oliveira RC, Gazzinelli G. Human schistosomiasis mansoni: immune responses during acute and chronic phases of the infection. Acta Trop 2008;108(2–3):109–17.
[8] Boros DL, Whitfield JR. Enhanced Th1 and dampened Th2 responses synergize to inhibit acute granulomatous and fibrotic responses in murine schistosomiasis mansoni. Infect Immun 1999;67(3):1187–93.
[9] Bonnard P, Remoue F, Schacht AM, Pialoux G, Riveau G. Association between serum cytokine profiles and schistosomiasis-related hepatic fibrosis: infection by *Schistosoma japonicum* versus *S. mansoni*. J Infect Dis 2006;193(5):748–9 author reply 9–50.
[10] Alves Oliveira LF, Moreno EC, Gazzinelli G, Martins-Filho OA, Silveira AM, Gazzinelli A, et al. Cytokine production associated with periportal fibrosis during chronic schistosomiasis mansoni in humans. Infect Immun 2006;74(2):1215–21.

[11] Jankovic D, Cheever AW, Kullberg MC, Wynn TA, Yap G, Caspar P, et al. CD4+ T cell-mediated granulomatous pathology in schistosomiasis is downregulated by a B cell-dependent mechanism requiring Fc receptor signaling. J Exp Med 1998;187(4): 619–29.
[12] Teixeira-Carvalho A, Martins-Filho OA, Peruhype-Magalhaes V, Silveira-Lemos D, Malaquias LC, Oliveira LF, et al. Cytokines, chemokine receptors, CD4+CD25HIGH+ T-cells and clinical forms of human schistosomiasis. Acta Trop 2008;108(2–3): 139–49.
[13] Ji F, Liu Z, Cao J, Li N, Liu Z, Zuo J, et al. B cell response is required for granuloma formation in the early infection of *Schistosoma japonicum*. PLoS One 2008;3(3): e1724.
[14] Dessein A, Chevillard C, Arnaud V, Hou X, Hamdoun AA, Dessein H, et al. Variants of CTGF are associated with hepatic fibrosis in Chinese, Sudanese, and Brazilians infected with schistosomes. J Exp Med 2009;206(11):2321–8.
[15] Burke ML, Jones MK, Gobert GN, Li YS, Ellis MK, McManus DP. Immunopathogenesis of human schistosomiasis. Parasite Immunol 2009;31(4):163–76.
[16] Elsammak MY, Al-Sharkaweey RM, Ragab MS, Amin GM, Kandil MH. In Egyptians, a mutation in the lymphotoxin-alpha gene may increase susceptibility to hepatitis C virus but not that to schistosomal infection. Ann Trop Med Parasitol 2008;102(8): 709–16.
[17] Deville WL, Buntinx F, Bouter LM, Montori VM, de Vet HC, van der Windt DA, et al. Conducting systematic reviews of diagnostic studies: didactic guidelines. BMC Med Res Methodol 2002;2:9.
[18] Laird NM, Lange C. Family-based designs in the age of large-scale gene-association studies. Nat Rev Genet 2006;7(5):385–94.
[19] Little J, Bradley L, Bray MS, Clyne M, Dorman J, Ellsworth DL, et al. Reporting, appraising, and integrating data on genotype prevalence and gene-disease associations. Am J Epidemiol 2002;156(4):300–10.
[20] Zintzaras E, Lau J. Synthesis of genetic association studies for pertinent gene-disease associations requires appropriate methodological and statistical approaches. J Clin Epidemiol 2008;61(7):634–45.
[21] Higgins JP, Thompson SG, Deeks JJ, Altman DG. Measuring inconsistency in meta-analyses. BMJ 2003;327(7414):557–60.
[22] Munafo MR, Flint J. Meta-analysis of genetic association studies. Trends Genet 2004;20(9):439–44.
[23] Perneger TV. What's wrong with Bonferroni adjustments. BMJ 1998;316(7139): 1236–8.
[24] Nakagawa S. A farewell to Bonferroni: the problems of low statistical power and publication bias. Behav Ecol 2004;15(6):1044–5.
[25] Peters JL, Sutton AJ, Jones DR, Abrams KR, Rushton L. Comparison of two methods to detect publication bias in meta-analysis. Jama 2006;295(6):676–80.
[26] Egger M, Davey Smith G, Schneider M, Minder C. Bias in meta-analysis detected by a simple, graphical test. BMJ 1997;315(7109):629–34.
[27] Begg CB, Mazumdar M. Operating characteristics of a rank correlation test for publication bias. Biometrics 1994;50(4):1088–101.
[28] Dessein AJ, Hillaire D, Elwali NE, Marquet S, Mohamed-Ali Q, Mirghani A, et al. Severe hepatic fibrosis in *Schistosoma mansoni* infection is controlled by a major locus that is closely linked to the interferon-gamma receptor gene. Am J Hum Genet 1999;65(3):709–21.
[29] Secor WE, del Corral H, dos Reis MG, Ramos EA, Zimon AE, Matos EP, et al. Association of hepatosplenic schistosomiasis with HLA-DQB1*0201. J Infect Dis 1996;174(5):1131–5.
[30] Assaad-Khalil SH, Helmy MA, Zaki A, Mikhail MM, el-Hai MA, el-Sawy M. Some genetic, clinical and immunologic interrelations in schistosomiasis mansoni. Ann Biol Clin (Paris) 1993;51(6):619–26.
[31] Hirayama K, Chen H, Kikuchi M, Yin T, Itoh M, Gu X, et al. Glycine-valine dimorphism at the 86th amino acid of HLA-DRB1 influenced the prognosis of postschistosomal hepatic fibrosis. J Infect Dis 1998;177(6):1682–6.
[32] Mohamed-Ali Q, Elwali NE, Abdelhameed AA, Mergani A, Rahoud S, Elagib KE, et al. Susceptibility to periportal (Symmers) fibrosis in human *Schistosoma mansoni* infections: evidence that intensity and duration of infection, gender, and inherited factors are critical in disease progression. J Infect Dis 1999;180(4): 1298–306.
[33] Dessein AJ, Marquet S, Henri S, El Wali NE, Hillaire D, Rodrigues V, et al. Infection and disease in human schistosomiasis mansoni are under distinct major gene control. Microbes Infect 1999;1(7):561–7.
[34] Eriksson J, Reimert CM, Kabatereine NB, Kazibwe F, Ireri E, Kadzo H, et al. The 434 (G>C) polymorphism within the coding sequence of Eosinophil Cationic Protein (ECP) correlates with the natural course of *Schistosoma mansoni* infection. Int J Parasitol 2007;37(12):1359–66.
[35] Cheng YL, Xu MX, Song WJ, Yang Y, Liu WQ, Li YL, et al. Microarray DNA chip in analyzing the association between HLA-DRB and advanced hepatosplenic schistosomiasis. Zhongguo Ji Sheng Chong Xue Yu Ji Sheng Chong Bing Za Zhi 2005;23(6):392–5.
[36] Blanton RE, Salam EA, Ehsan A, King CH, Goddard KA. Schistosomal hepatic fibrosis and the interferon gamma receptor: a linkage analysis using single-nucleotide polymorphic markers. Eur J Hum Genet 2005;13(5):660–8.
[37] Zhang JH, Liu WQ, Li YL, Long XC. Studies on the association of human leukocyte antigen class II alleles with advanced hepatosplenic schistosomiasis japonica. Zhongguo Ji Sheng Chong Xue Yu Ji Sheng Chong Bing Za Zhi 2005;23(1):6–9.
[38] Chevillard C, Moukoko CE, Elwali NE, Bream JH, Kouriba B, Argiro L, et al. IFN-gamma polymorphisms (IFN-gamma +2109 and IFN-gamma +3810) are associated with severe hepatic fibrosis in human hepatic schistosomiasis (*Schistosoma mansoni*). J Immunol 2003;171(10):5596–601.
[39] Moukoko CE, El Wali N, Saeed OK, Mohamed-Ali Q, Gaudart J, Dessein AJ, et al. No evidence for a major effect of tumor necrosis factor alpha gene polymorphisms in periportal fibrosis caused by *Schistosoma mansoni* infection. Infect Immun 2003;71(10):5456–60.
[40] Hirayama K. Genetic factors associated with development of cerebral malaria and fibrotic schistosomiasis. Korean J Parasitol 2002;40(4):165–72.
[41] McManus DP, Ross AG, Williams GM, Sleigh AC, Wiest P, Erlich H, et al. HLA class II antigens positively and negatively associated with hepatosplenic schistosomiasis in a Chinese population. Int J Parasitol 2001;31(7):674–80.
[42] Hirayama K, Chen H, Kikuchi M, Yin T, Gu X, Liu J, et al. HLA-DR-DQ alleles and HLA-DP alleles are independently associated with susceptibility to different stages of post-schistosomal hepatic fibrosis in the Chinese population. Tissue Antigens 1999;53(3):269–74.
[43] Waine GJ, Ross AG, Williams GM, Sleigh AC, McManus DP. HLA class II antigens are associated with resistance or susceptibility to hepatosplenic disease in a Chinese population infected with *Schistosoma japonicum*. Int J Parasitol 1998;28(4): 537–42.
[44] Hafez M, Aboul Hassan S, el-Tahan H, el-Shennawy F, Khashaba M, al-Tonbary Y, et al. Immunogenetic susceptibility for post-schistosomal hepatic fibrosis. Am J Trop Med Hyg 1991;44(4):424–33.
[45] Cabello PH, Krieger H, Lopes JD, Sant'Ana EJ. On the association between HLA-A1 and B5 and clinical forms of schistosomiasis mansoni. Mem Inst Oswaldo Cruz 1991;86(1):37–40.
[46] Abdel-Salam E, Abdel Khalik A, Abdel-Meguid A, Barakat W, Mahmoud AA. Association of HLA class I antigens (A1, B5, B8 and CW2) with disease manifestations and infection in human schistosomiasis mansoni in Egypt. Tissue Antigens 1986;27(3):142–6.
[47] Wang CG, Zhu QY, Hang PY, Zhu YW, Wang JW, Shen YP, et al. HLA and schistosomiasis japonica. Chin Med J (Engl) 1984;97(8):603–5.
[48] El-Tayeb S, Nasr E, Soliman S. HLA and bilharzial liver disease. J Haematol 1982;7: 1–5.
[49] Salam EA, Ishaac S, Mahmoud AA. Histocompatibilty-linked susceptibility for hepatospleenomegaly in human schistosomiasis mansoni. J Immunol 1979;123(4): 1829–31.
[50] The use of diagnostic ultrasound in schistosomiasis – attempts at standardization of methodology. Cairo Working Group. Acta Trop 1992;51(1):45–63.
[51] Grubic Z, Zunec R, Peros-Golubicic T, Tekavec-Trkanjec J, Martinez N, Alilovic M, et al. HLA class I and class II frequencies in patients with sarcoidosis from Croatia: role of HLA-B8, -DRB1*0301, and -DQB1*0201 haplotype in clinical variations of the disease. Tissue Antigens 2007;70(4):301–6.
[52] Harraga S, Godot V, Bresson-Hadni S, Mantion G, Vuitton DA. Profile of cytokine production within the periparasitic granuloma in human alveolar echinococcosis. Acta Trop 2003;85(2):231–6.
[53] Martinetti M, Tinelli C, Kolek V, Cuccia M, Salvaneschi L, Pasturenzi L, et al. "The sarcoidosis map": a joint survey of clinical and immunogenetic findings in two European countries. Am J Respir Crit Care Med 1995;152(2):557–64.
[54] Hue S, Cacoub P, Renou C, Halfon P, Thibault V, Charlotte F, et al. Human leukocyte antigen class II alleles may contribute to the severity of hepatitis C virus-related liver disease. J Infect Dis 2002;186(1):106–9.
[55] Yu RB, Hong X, Ding WL, Tan YF, Zhang YX, Sun NX, et al. The association between the genetic polymorphism of HLA-DQA1, DQB1, and DRB1 and serum alanine aminotransferase levels in chronic hepatitis C in the Chinese population. J Gastroenterol Hepatol 2008;23(9):1394–402.
[56] Sharma SK, Balamurugan A, Saha PK, Pandey RM, Mehra NK. Evaluation of clinical and immunogenetic risk factors for the development of hepatotoxicity during antituberculosis treatment. Am J Respir Crit Care Med 2002;166(7):916–9.
[57] Jores RD, Frau F, Cucca F, Grazia Clemente M, Orru S, Rais M, et al. HLA-DQB1*0201 homozygosis predisposes to severe intestinal damage in celiac disease. Scand J Gastroenterol 2007;42(1):48–53.
[58] Caillat-Zucman S, Garchon HJ, Timsit J, Assan R, Boitard C, Djilali-Saiah I, et al. Age-dependent HLA genetic heterogeneity of type 1 insulin-dependent diabetes mellitus. J Clin Invest 1992;90(6):2242–50.
[59] Reveille JD, Macleod MJ, Whittington K, Arnett FC. Specific amino acid residues in the second hypervariable region of HLA-DQA1 and DQB1 chain genes promote the Ro (SS-A)/La (SS-B) autoantibody responses. J Immunol 1991;146(11):3871–6.
[60] Pereira LM, McFarlane BM, Massarolo P, Saleh MG, Bridger C, Spinelli V, et al. Specific liver autoreactivity in schistosomiasis mansoni. Trans R Soc Trop Med Hyg 1997;91(3):310–4.
[61] Peng S, Trimble C, Wu L, Pardoll D, Roden R, Hung CF, et al. HLA-DQB1*02-restricted HPV-16 E7 peptide-specific CD4+ T-cell immune responses correlate with regression of HPV-16-associated high-grade squamous intraepithelial lesions. Clin Cancer Res 2007;13(8):2479–87.
[62] Migot-Nabias F, Fajardy I, Danze PM, Everaere S, Mayombo J, Minh TN, et al. HLA class II polymorphism in a Gabonese Banzabi population. Tissue Antigens 1999;53(6): 580–5.
[63] Abdennaji Guenounou B, Loueslati BY, Buhler S, Hmida S, Ennafaa H, Khodjet-Elkhil H, et al. HLA class II genetic diversity in southern Tunisia and the Mediterranean area. Int J Immunogenet 2006;33(2):93–103.
[64] Chen S, Hu Q, Xie Y, Zhou L, Xiao C, Wu Y, et al. Origin of Tibeto-Burman speakers: evidence from HLA allele distribution in Lisu and Nu inhabiting Yunnan of China. Hum Immunol 2007;68(6):550–9.
[65] Trachtenberg E, Vinson M, Hayes E, Hsu YM, Houtchens K, Erlich H, et al. HLA class I (A, B, C) and class II (DRB1, DQA1, DQB1, DPB1) alleles and haplotypes in the Han from southern China. Tissue Antigens 2007;70(6):455–63.
[66] Satoh M, Toma H, Sato Y, Kikuchi M, Takara M, Shiroma Y, et al. Production of a high level of specific IgG4 antibody associated with resistance to albendazole treatment in HLA-DRB1*0901-positive patients with strongyloidiasis. Am J Trop Med Hyg 1999;61(4):668–71.

[67] Neild GH, Rodriguez-Justo M, Wall C, Connolly JO. Hyper-IgG4 disease: report and characterisation of a new disease. BMC Med 2006;4:23.
[68] Silveira AM, Bethony J, Gazzinelli A, Kloos H, Fraga LA, Alvares MC, et al. High levels of IgG4 to *Schistosoma mansoni* egg antigens in individuals with periportal fibrosis. Am J Trop Med Hyg 2002;66(5):542–9.
[69] Abel LC, Iwai LK, Viviani W, Bilate AM, Fae KC, Ferreira RC, et al. T cell epitope characterization in tandemly repetitive *Trypanosoma cruzi* B13 protein. Microbes Infect 2005;7(11–12):1184–95.
[70] Hernandez-Pacheco G, Aguilar-Garcia J, Flores-Dominguez C, Rodriguez-Perez JM, Perez-Hernandez N, Alvarez-Leon E, et al. MHC class II alleles in Mexican patients with rheumatic heart disease. Int J Cardiol 2003;92(1):49–54.
[71] Brouwer MC, de Gans J, Heckenberg SG, Zwinderman AH, van der Poll T, van de Beek D. Host genetic susceptibility to pneumococcal and meningococcal disease: a systematic review and meta-analysis. Lancet Infect Dis 2009;9(1):31–44.
[72] Duarte-Rey C, Pardo AL, Rodriguez-Velosa Y, Mantilla RD, Anaya JM, Rojas-Villarraga A. HLA class II association with autoimmune hepatitis in Latin America: a meta-analysis. Autoimmun Rev 2009;8(4):325–31.
[73] Castano-Rodriguez N, Diaz-Gallo LM, Pineda-Tamayo R, Rojas-Villarraga A, Anaya JM. Meta-analysis of HLA-DRB1 and HLA-DQB1 polymorphisms in Latin American patients with systemic lupus erythematosus. Autoimmun Rev 2008;7(4):322–30.
[74] Yang YC, Chang TY, Lee YJ, Su TH, Dang CW, Wu CC, et al. HLA-DRB1 alleles and cervical squamous cell carcinoma: experimental study and meta-analysis. Hum Immunol 2006;67(4–5):331–40.

Mitochondrion 11 (2011) 273–278

Contents lists available at ScienceDirect

Mitochondrion

journal homepage: www.elsevier.com/locate/mito

Concatenated mitochondrial DNA of the coccidian parasite *Eimeria tenella*

Kenji Hikosaka [a], Yutaka Nakai [b], Yoh-ichi Watanabe [c], Shin-Ichiro Tachibana [a], Nobuko Arisue [d], Nirianne Marie Q. Palacpac [d], Tomoko Toyama [a,d], Hajime Honma [a,e], Toshihiro Horii [d], Kiyoshi Kita [c], Kazuyuki Tanabe [a,*]

[a] *Laboratory of Malariology, International Research Center of Infectious Diseases, Research Institute for Microbial Diseases, Osaka University, Suita, Osaka 565-0871, Japan*
[b] *Laboratory of Sustainable Environmental Biology, Graduate School of Agricultural Science, Tohoku University, Osaki, Miyagi 989-6711, Japan*
[c] *Department of Biomedical Chemistry, Graduate School of Medicine, The University of Tokyo, Bunkyo-ku, Tokyo 113-0033, Japan*
[d] *Department of Molecular Protozoology, Research Institute for Microbial Diseases, Osaka University, Suita, Osaka 565-0871, Japan*
[e] *Japan Society for the Promotion of Science, Japan*

ARTICLE INFO

Article history:
Received 28 June 2010
Received in revised form 12 October 2010
Accepted 25 October 2010
Available online 31 October 2010

Keywords:
Mitochondrion
Mitochondrial genome
Eimeria
Plasmodium
Apicomplexa
Nuclear mitochondrial DNA

ABSTRACT

Apicomplexan parasites of the genus *Plasmodium*, pathogens causing malaria, and the genera *Babesia* and *Theileria*, aetiological agents of piroplasmosis, are closely related. However, their mitochondrial (mt) genome structures are highly divergent: *Plasmodium* has a concatemer of 6-kb unit and *Babesia/Theileria* a monomer of 6.6- to 8.2-kb with terminal inverted repeats. Fragmentation of ribosomal RNA (rRNA) genes and gene arrangements are remarkably distinctive. To elucidate the evolutionary origin of this structural divergence, we determined the mt genome of *Eimeria tenella*, pathogens of coccidiosis in domestic fowls. Analysis revealed that *E. tenella* mt genome was concatemeric with similar protein-coding genes and rRNA gene fragments to *Plasmodium*. Copy number was 50-fold of the nuclear genome. Evolution of structural divergence in the apicomplexan mt genomes is discussed.

1. Introduction

Mitochondria, organelles essential for a range of cellular processes and cellular signaling, are ubiquitous in all eukaryotes. Mitochondrial (mt) genomes exhibit remarkable variation in structure and size (Gray et al., 2004), from the 6-kb genome in the malaria parasite *Plasmodium* (Feagin, 1992) to the large (180 to 2400 kb) mt genome in land plants (Ward et al., 1981; Palmer et al., 1992). *Plasmodium* belongs to the phylum Apicomplexa, with more than 5000 species, all clinically and/or economically important pathogens (Levine, 1988): *Eimeria*, responsible for the diseases of intestinal coccidiosis in intensively reared livestock; *Toxoplasma*, etiological agent of toxoplasmosis in immune-compromised patients and congenitally infected fetuses; *Cryptosporidium*, pathogens for cryptosporidiosis in humans and animals; *Babesia*, causing babesiosis in ruminants and humans; and *Theileria*, causal agents of tropical theileriosis and East Coast fever in cattle.

Mt genomes of a few apicomplexan genera have been studied, and available data suggest that they are remarkably diverse in structure and genome organization. The minuscule 6-kb tandemly repeated linear or concatenated mtDNA of *Plasmodium* encodes only three protein-coding genes (cytochrome *c* oxidase subunits I [*cox1*] and III [*cox3*] and cytochrome *b* [*cob*]) in addition to large subunit (LSU) and small subunit (SSU) ribosomal RNA (rRNA) genes (Preiser et al., 1996). The two rRNA genes are highly fragmented with 19 identified rRNA pieces (Feagin et al., 1997). The arrangement of these mt genes is completely conserved in the genus (Perkins, 2008). In the genera of *Babesia* and *Theileria*, known as piroplasms, closely related to *Plasmodium* (Lau, 2009), the mt genomes are monomeric linear, from 6.6 kb to 8.2 kb, with terminal inverted repeats on both ends (Kairo et al., 1994; Hikosaka et al., 2010). Although the *Babesia/Theileria* mt genomes encode the same three protein-coding genes, gene array and transcriptional direction are different. Furthermore, only six fragmented LSU have been identified in the *Babesia/Theileria* mt genomes, with fragmentation different from that of *Plasmodium*. Thus, the mt genomes of *Plasmodium* and *Babesia/Theileria* are structurally highly divergent regardless of their close relatedness. Although the mt genome of *Toxoplasma gondii* has yet to be sequenced, multiple copies of partial mt genes (*cox1* and *cob*) were found to be scattered throughout the nuclear genome (Ossorio et al., 1991). In *Cryptosporidium*, the mitochondrion is reduced to mitosome and has no DNA (Mogi and Kita, 2010). The phylum Apicomplexa, therefore, encompasses a large number of interesting genera to further understand the evolution of mt genomes.

* Corresponding author. Laboratory of Malariology, International Research Center of Infectious Diseases, Research Institute for Microbial Diseases, Osaka University, 3-1 Yamadaoka, Suita, Osaka 565-0871, Japan. Tel.: +81 6 6879 4260; fax: +81 6 6879 4262.
E-mail address: kztanabe@biken.osaka-u.ac.jp (K. Tanabe).

1567-7249/$ – see front matter © 2010 Elsevier B.V. and Mitochondria Research Society. All rights reserved.
doi:10.1016/j.mito.2010.10.003

In Apicomplexa, *Plasmodium* and *Babesia/Theileria* belong to the class Haematozoea, and *Eimeria* and other intestinal coccidian parasites including *Toxoplasma* belong to the class Coccidea (Hausmann and Hülsmann, 1996). The genus *Eimeria* undergoes all of its developmental stages in one host, whereas parasites belonging to the class Haematozoea require two hosts to complete their life cycles, namely, the sexual development in invertebrate vectors and the asexual development in vertebrate host. Coccidian parasites have, nevertheless, complex developmental cycles: first, oocysts excreted from the hosts undergo differentiation (sporulation) in the environment and become infective. When ingested by a host animal, oocysts undergo rounds of discrete, expansive asexual reproduction (merogony and schizogony) in the intestine, followed by sexual differentiation, fertilization and shedding of unsporulated oocysts (Jeurissen et al., 1996). *Eimeria tenella* is one of the most important *Eimeria* species, as it causes intestinal coccidiosis in domestic fowls (*Gallus gallus*), imposing enormous economic losses (Shirley et al., 2004). In *E. tenella*, two extrachromosomal DNAs have been demonstrated by pulsed-field gel electrophoresis (Dunn et al., 1998): one is the 35 kb apicoplast genome (Cai et al., 2003) and the other is a smaller size mt genome. The primary structure and the gene organization of *E. tenella* mt genome, however, remain undetermined. In this study, we report the mt genome sequence of *E. tenella*, and show that the *E. tenella* mt genome has the form of a tandemly repeated linear element or concatemer structure, and contains 19 rRNA fragments as well as three protein-coding genes. This finding indicates that the mt genomes of both *Eimeria* and *Plasmodium* retain common structural features. We discuss evolution of structural divergence in the apicomplexan mt genomes. Additionally, we identified nuclear genome DNA fragments that are shared by the mt genome of *E. tenella*.

2. Materials and methods

2.1. Blast search for mt genome sequence

A contig of *Eimeria tenella* (Houghton strain), containing mtDNA, was retrieved from *Eimeria tenella* GeneDB (http://www.genedb.org/Homepage/Etenella) using the following gene names: cytochrome *c* oxidase subunit 1, cytochrome *c* oxidase subunit 3 and cytochrome *b*. Two unfinished genomic sequences (EIMER_contig_00018071 and EIMER_contig_00018452), encoding putative COX1 and putative COB, respectively, were obtained from the Wellcome Trust Sanger Institute (http://www.sanger.ac.uk/Projects/E_tenella/).

2.2. DNA sequencing

E. tenella NIAH strain was maintained at Tohoku University by routine passage through chickens. Oocyst stage parasites were collected from feces of infected chickens and purified by the centrifugation method (Nakai et al., 1993). Purified oocysts were subjected to 5 times repeated freeze–thawing. Parasite genomic DNA was isolated using QIAamp DNA Blood Mini Kit (QIAGEN, Hilden, Germany). Genomic DNA of *Plasmodium gallinaceum* (8A strain) was kindly provided by the late M. Shahabuddin (NIAID/NIH, USA). Nucleotide sequences of the *E. tenella* mt genome; small subunit (SSU) and large subunit (LSU) rRNA genes of the *E. tenella* apicoplast genome; *cox1* and *cob* of the *P. gallinaceum* mt genome were determined by direct sequencing of polymerase chain reaction (PCR) products using specific primers (Supplementary Table 1A) designed from retrieved sequences. Amplification conditions, PCR product purification (QIAquick PCR purification kit, QIAGEN) and DNA sequencing of two independent PCR products were carried out as previously described (Hikosaka et al., 2010). Sequencing primers were designed to cover target regions in both directions. The sequences obtained in this study have been deposited in DDBJ/EMBL/GenBank with the following accession numbers: AB564272 to AB564276.

2.3. Gene annotation

Nucleotide sequences of *E. tenella* were aligned with reported sequences from *P. falciparum* (GenBank accession # M76611), *P. mexicanum* (EF079653), *B. bovis* (AB499088), *T. parva* (AB499089) and *T. annulata* (NW_001091933) by CLUSTAL W (Thompson et al., 1994) with manual corrections. Protein-coding genes were predicted using previously annotated sequences from the five parasite species. Putative rRNA genes were identified essentially as described (Hikosaka et al., 2010). MtDNA sequence or annotated rRNA gene fragments from *P. falciparum* (M76611) were used as query under suggested algorithm parameters (Freyhult et al., 2007) in NCBI BLAST 2.2 (Altschul et al., 1990). The termini of the candidate genes were assigned using aligned sequences and putative base-pairings between fragments proposed for *P. falciparum* mt rRNA fragments, and secondary structure predicted by CentroidHomfold (Hamada et al., 2009).

2.4. Southern blot hybridization

Genomic DNA of *E. tenella*, either undigested or digested with *Hind*III or *Pvu*II, were electrophoresed on 1.0% agarose gels in TAE (40 mM Tris–acetate, 1 mM EDTA) and transferred to a positively charged nylon membrane (Amersham Hybond-N+, GE Healthcare, Little Chalfont, England). PCR products specifically amplified for target regions of the *E. tenella* mt genome were labeled with digoxigenin-dUTP using the DIG High Prime DNA Labeling and Detection Starter Kit II (Roche Diagnostics, Rotkreuz, Switzerland). After overnight hybridization with the DIG-labeled DNA probes, blots were washed twice with 2× SSC, 0.1% SDS and twice with 0.5× SSC, 0.1% SDS, at 65 °C for 15 min. Hybridization signals were detected using Detection Starter Kit II. Southern blot hybridization was also done in parallel with *P. falciparum*, whose mt genome structure is known to be circular or linear concatenated with numerous branching off (Preiser et al., 1996).

2.5. Phylogenetic analysis

The concatenated amino acid sequences of COX1 and COB (755 sites) from 15 apicomplexan parasites (Supplementary Table 2) were used for phylogenetic analysis. A free-living ciliate, *Tetrahymena thermophila* (Brunk et al., 2003), was included as an outgroup. COX3 was not used, since *cox3* of *T. thermophila* is present in the nuclear (but not mt) genome. We constructed the maximum likelihood (ML) phylogenetic trees by the PROML program in PHYLIP version 3.68 (Felsenstein and Churchill, 1996). CODEML program in PAML version 4.2 (Yang, 2007) was used to estimate the Γ shape parameter value α. Bootstrap analysis was done by applying PROML to 100 re-sampled datasets produced by SEQBOOT program in PHYLIP.

A phylogenetic tree of LSU sequences of the mt genomes (LSUE, LSUF, LSUG and RNA10, 379 sites in total) was constructed using the ML method implemented in PAUP* 4.0 b10 (Swofford, 2002). SSU/LSU sequences of the apicoplast genomes (3045 sites) (Supplementary Table 2) were also used for phylogenetic analysis. The non-photosynthetic flagellate, *Astasia longa*, was included as an outgroup instead of *T. thermophila* which lacks a plastid genome. Bootstrap probability was estimated from 1000 heuristic replicates. For statistical comparisons among the best-tree and its alternatives, p-values of the KH test (Kishino and Hasegawa, 1989), the SH test (Shimodaira and Hasegawa, 1999) and the AU test (Shimodaira, 2002) were obtained.

2.6. Search for nuclear mitochondrial DNA in E. tenella

In some eukaryotes, nuclear genomes contain DNA segments which have a high sequence similarity to mtDNA (Caro et al., 2010; Hazkani-Covo et al., 2010). These sequences are considered to have been derived from mtDNA and thus designated as nuclear mtDNAs

(NUMTs) (Richly and Leister, 2004). The contigs (File version; assembly 2007_05_08.gz) of *E. tenella* were retrieved from the Wellcome Trust Sanger Institute, and the whole mt sequence obtained in this study was used as query under cut-off conditions of >50 nucleotides and >95% identity. We identified 21 NUMTs and confirmed these by direct sequencing (Supplementary Table 3). Two NUMTs, Emt3 and Emt4 occurring in contigs 00028951 and 00029260, respectively (Supplementary Table 1B), were used for Southern blot hybridization analysis against *E. tenella* DNA. Copy number of *E. tenella* mt genome was estimated using dot blot hybridization. Briefly, DNA fragments of the mt genome and the contig (contig_00029260) were amplified by PCR using specific primers (Supplementary Table 1C), and DNA amount was measured. Serial known dilutions of control PCR products were dot-blotted onto a nylon membrane, following heat denaturation (99 °C, 10 min). Genomic DNA were electrophoresed on agarose gels and then transferred to a nylon membrane. A PCR product specifically amplified from target regions of the *E. tenella* mt genome (Supplementary Table 1B) was labeled as described. Chemiluminescence signals were quantitated using LAS-4000mini.

3. Results and discussion

3.1. Mitochondrial genome organization

We obtained a mt genome sequence (6213 bp) from *E. tenella*, in which three protein-coding genes, *cob*, *cox1* and *cox3*, and 12 fragments of the large subunit (LSU) rRNA gene and 7 fragments of the small subunit (SSU) rRNA gene were identified (Fig. 1A). These genes and rRNA gene fragments are also present in the *P. falciparum* (Fig. 1B) (Feagin et al., 1997), although gene arrangements greatly differ between the two mt genomes.

Southern blot hybridization with a *cox3* probe (Emt1) against undigested DNA produced a smeared signal from around 4 kb to 20 kb. Hybridization against DNA digested with *Hind*III gave a major band at 6.2 kb which tailed-off to lower contiguous fragments. Hybridization against DNA digested with *Pvu*II yielded a clear signal at 2.6 kb. These signal sizes matched to those predicted from the *E. tenella* mt sequence (Fig. 2A and C). A *cox1* probe (Emt2) gave similar results (not shown). Southern blot hybridization using a *P. falciparum* probe (Pmt1) revealed a smeared signal from 6 kb to 23 kb against *P. falciparum* undigested DNA, a distinct band at 1.3 kb against *Hind*III-digested DNA, and a predominant 6.0 kb single band which tailed-off to a smear against *Pvu*II-digested DNA (Fig. 2B and D); yielding a similar hybridization pattern to *E. tenella*. This suggests that the *E. tenella* mt genome structure is similar to that of *P. falciparum*. The long tailing-off smears observed in both *E. tenella* and *P. falciparum* were not found in the mt genomes of *Babesia* and *Theileria* (Hikosaka et al., 2010), which have monomeric linear structures. The tailing-off smears probably reflect DNA fragments of various sizes branching off from polydispersed linear DNA molecules with various length termini (Preiser et al., 1996), which seems to be characteristics of a polydispersed concatenated mtDNA. In *E. tenella*, this tailing was somewhat longer than in *P. falciparum*, probably due to fragmentation caused by repeated freeze–thawing to disrupt the oocyst wall, which is highly rigid and not permeable to common solvents used for disruption. The absence of specific restriction fragments smaller than 6.2 kb after digestion with single-site enzymes suggests that the ends of the linear concatemers are not defined by telomere-like unique sequences, as seen in *Babesia* and *Theileria* (Kairo et al., 1994; Hikosaka et al., 2010). These results strongly suggest that the bulk of *E. tenella* mtDNA consist of polydisperse head-to-tail tandem arrays of the 6.2 kb element as in *P. falciparum*.

3.2. Phylogeny

The ML tree of concatenated COX1 and COB amino acid sequences revealed monophyly of the genera *Babesia* and *Theileria*, and of the genus *Plasmodium* with high BP values of 98 and 89%, respectively (Fig. 3A). *E. tenella* was positioned close to *Plasmodium* with a moderate BP value (75%). The ML tree of LSU sequences showed the same topology to that of the *cox1+cob* tree (Supplementary Fig. 1): *E. tenella* positioned close to *Plasmodium* with a low BP value (55%). ML tree using SSU and LSU sequences of the apicoplast genome, however, yielded a topology with *E. tenella* and *T. gondii* branching off from a common ancestor of *Plasmodium* and *Babesia/Theileria* with 100% BP (Fig. 3B). Thus, topologies of the mt trees and the apicoplast tree are not consistent. The inconsistency was not due to differences in the number of taxa used for tree construction because BP value changed little (76%) even when the number of taxa in the *cox1+cob* tree was reduced to the same as the apicoplast tree (data not shown).

The two mt tree topologies are also not consistent with phylogenetic trees constructed using 18S rRNA gene or hundreds of protein-coding nuclear genes (Morrison and Ellis, 1997; Philippe et al., 2004; Kuo et al., 2008), whereas the apicoplast tree is consistent with trees of nuclear genes. Since the positions of *E. tenella* in the two mt trees were not well supported with high BP values, we tested other possibilities of *E. tenella* position. The KH, the SH or the AU tests did not reject these alternative positions of *E. tenella* placed at a common ancestor of *Plasmodium* and *Babesia/Theileria* (arrow a in Fig. 3A) or at a common ancestor of *Babesia/Theileria* (arrow b in Fig. 3A) (Supplementary Table 4). Phylogenetic position of *E. tenella*, thus, remains unresolved with the mt dataset. *Eimeria* and other intestinal coccidians belong to the class Coccidea, and *Plasmodium* and *Babesia/Theileria* belong to the class Haematozoea. The two classes show remarkably different life cycles (Hausmann and Hülsmann, 1996). This taxonomical classification is consistent with phylogenetic trees

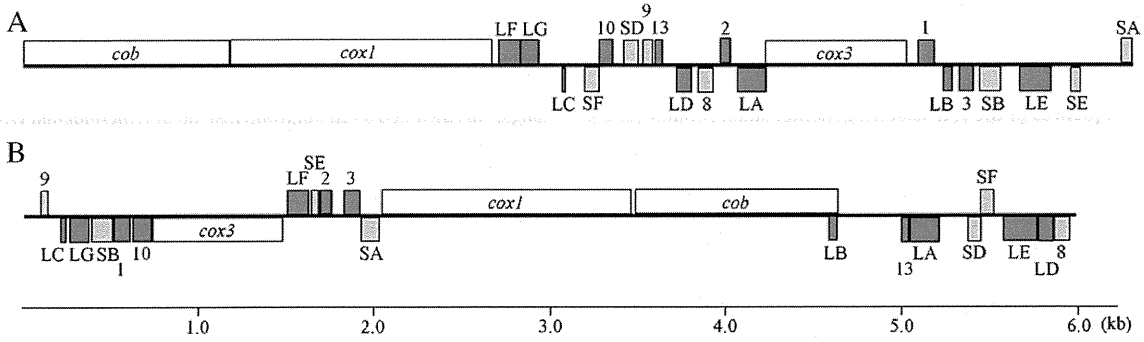

Fig. 1. Mitochondrial genome structure of *Eimeria tenella* (A) and *Plasmodium falciparum* (B). Genes shown above the bold line in each genome have predicted transcriptional directions from left to right; and those below, from right to left. Because the 6.2 kb element of *E. tenella* mt genome is tandemly repeated, both termini are arbitrary. For details refer to GenBank accession numbers AB564272 and M76611. White boxes indicate protein-coding genes (*cox1*, *cox3* and *cob*); fragments of LSU (LA–LG, 1, 2, 3, 10 and 13) and SSU (SA, SB, SD–SF, 8 and 9) rRNA genes are shown by dark and light gray boxes, respectively.

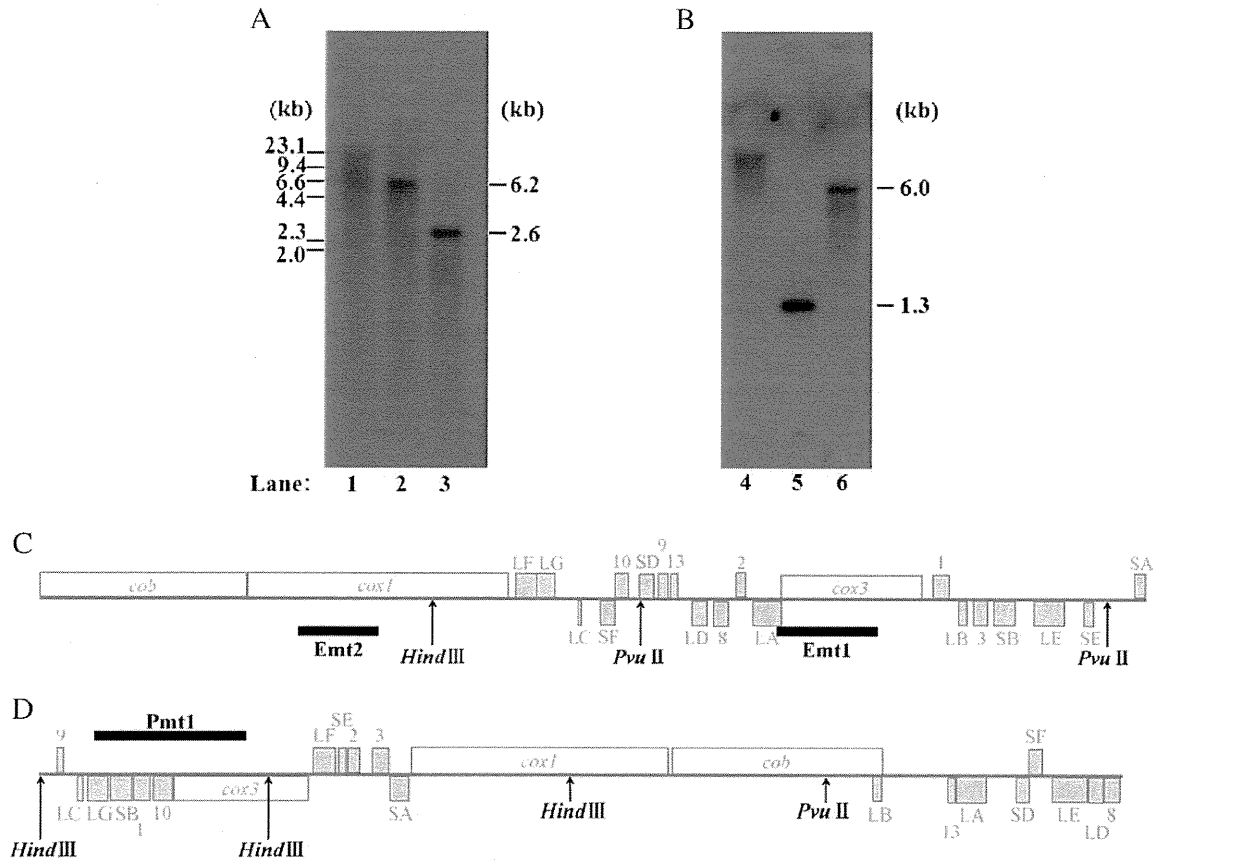

Fig. 2. Southern blot hybridization showing the mitochondrial (mt) genomes of *Eimeria tenella* (A) and *Plasmodium falciparum* (B). *E. tenella* probes (Emt1 and Emt2) and a *P. falciparum* probe (Pmt1), whose positions are shown in (C) and (D), were hybridized against undigested DNA of *E. tenella* and *P. falciparum*, respectively (lanes 1 and 4) and DNA digested with *Hind*III (lanes 2 and 5) or *Pvu*II (lanes 3 and 6).

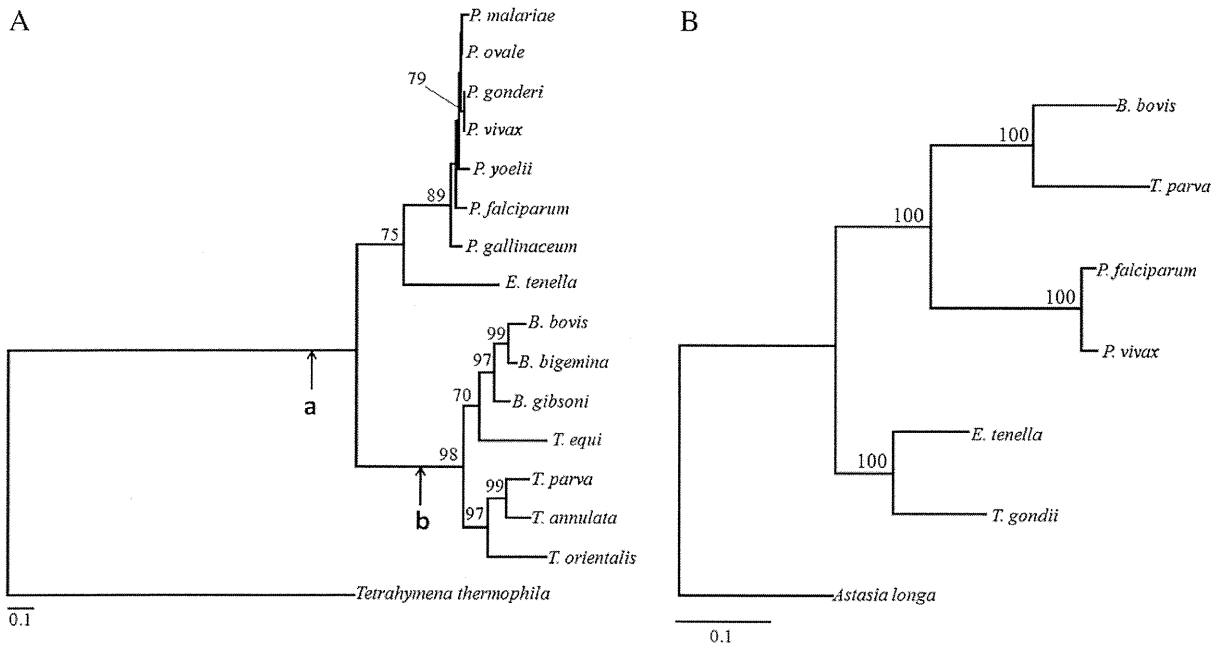

Fig. 3. Maximum likelihood phylogenetic trees of mitochondrial genes, *cox1* and *cob*, from *Plasmodium*, *Eimeria tenella*, *Babesia* and *Theileria* with *Tetrahymena thermophila* as an outgroup (A); and of apicoplast small and large subunits (SSU and LSU) of rRNA genes from six apicomplexan species with *Astasia longa* as an outgroup (B). For *cox1*+*cob* tree, concatenated amino acid sequences (755 sites) were used with 1000 heuristic replicates under a Jones, Taylor, and Thornton model (Jones et al., 1992) ($\alpha = 0.86$). For apicoplast SSU+LSU tree, concatenated nucleotide sequences (3045 sites in total: 1037 bp for SSU; 2008 bp for LSU) were used with 1000 heuristic replicates under a GTR+Γ model ($\alpha = 1.22$). Numbers shown along nodes represent bootstrap values. Arrows a and b indicate alternative positions of *E. tenella*. Both possibilities were statistically compared by the SH, KH and AU tests.

constructed using nuclear genes (Morrison and Ellis, 1997; Philippe et al., 2004; Kuo et al., 2008) and the apicoplast genome tree (Fig. 3B). We therefore consider it likely that *E. tenella* branched off from a common ancestor of *Plasmodium* clade and *Babesia/Theileria* clade.

Adopting this phylogenetic relationship allows us to infer a scenario for evolutionary trajectory of the mt genome structure of apicomplexans. Since both *Eimeria* and *Plasmodium* possess concatenated mtDNA, a common ancestor of these two parasites might have had a concatenated form of the mt genome, and the monomeric linear mt genomes of *Babesia/Theileria* were generated in the lineage. The present finding that *Eimeria* has the same 19 rRNA gene fragments as seen in the *Plasmodium* mt genome supports this scenario. Although we favor this scenario, we cannot completely rule out the possibility that a monomeric linear structure was an ancestral form and concatenated genome structures of *Eimeria* and *Plasmodium* evolved independently in each lineage. The likelihood is supported by *Tetrahymena* which has linear mt genomes, similar to those found in mt genomes of *Babesia/Theileria*. However, evolutionary distance between *Tetrahymena* and Apicomplexa is too far to gain insights into an ancestral form of the apicomplexan mt genome and, likewise, changes in molecular architecture of mt genomes are very frequent (Nosek and Tomaska, 2003). Nevertheless, it should be noted that mt genome architecture is conserved and does not change frequently within genus of the phylum: thus, in apicomplexan mt genome sequences available to date, all eight *Babesia/Theileria* species have the form of linear structure (Hikosaka et al., 2010), and all 23 *Plasmodium* species have the form of concatemer structure (Hikosaka et al., unpublished data). This within-genus stability of mt genome structure should allow us to infer an ancestral form of the apicomplexan mt genomes. In order to clarify evolutionary trajectory of the mt genome of Apicomplexa, further analysis of mt genomes of algae, closely related to apicomplexans such as *Chromera velia* and CCMP3155 (an undescribed species) would be required (Janouskovec et al., 2010).

3.3. Nuclear mitochondrial DNAs (NUMTs) in E. tenella

Blast search identified 21 sequence segments similar to the *E. tenella* mtDNA with lengths from 51 to 146 nucleotides in the *E. tenella* contigs (Supplementary Table 5). In contigs containing multiple NUMTs, several NUMTs were found arrayed in direct junction or in close proximity. Southern blot hybridization using probes Emt3 and Emt4, which contain NUMTs, gave signals derived from the *E. tenella* mt genome. We were, however, unable to detect signals derived from the nuclear genome by a similar procedure (Supplementary Fig. 2). In contrast, a probe specific to the nuclear genome (Enu1) hybridized at predicted sizes against either undigested DNA or DNA digested with *HindIII* or *Eco*RI, when a large amount of gDNA was used (data not shown). Copy number estimation analysis using Southern hybridization showed that *E. tenella* cells contained around 50 copies of the 6.2 kb element per haploid nuclear genome. The failure of detecting NUMTs in the nuclear genome with Emt3 and Emt4 was thus likely due to this copy number difference, with potential signals from the nuclear genome being masked in a smear of mtDNA.

4. Conclusion

This study suggests that the mt genome of ancestral apicomplexan parasites had a concatenated structure containing 19 rRNA gene fragments as well as three protein-coding genes and that the monomeric linear mt genome of *Babesia/Theileria* was generated in the lineage of the genera. Elucidation of a molecular mechanism, by which a linear mt genome with terminal inverted repeats on both ends was established, should help to further understand the evolution and divergence of mt genomes.

Supplementary data to this article can be found online at doi:10.1016/j.mito.2010.10.003.

Acknowledgements

This work was supported by Grant-in-Aids for Scientific Research from the Ministry of Education, Culture, Sports, Science and Technology of Japan (18073013) and from Japan Society for Promotion of Sciences (18GS03140013 and 20390120). We would like to thank the *Eimeria tenella* genome project at the Sanger Institute, UK (http://www.sanger.ac.uk/Projects/E_tenella) for partial sequences in the design of some PCR primers.

References

Altschul, S.F., Gish, W., Miller, W., Myers, E.W., Lipman, D.J., 1990. Basic local alignment search tool. J. Mol. Biol. 215 (3), 403–410.
Brunk, C.F., Lee, L.C., Tran, A.B., Li, J., 2003. Complete sequence of the mitochondrial genome of *Tetrahymena thermophila* and comparative methods for identifying highly divergent genes. Nucleic Acids Res. 31 (6), 1673–1682.
Cai, X., Fuller, A.L., McDougald, L.R., Zhu, G., 2003. Apicoplast genome of the coccidian *Eimeria tenella*. Gene 321, 39–46.
Caro, P., Gomez, J., Arduini, A., Gonzalez-Sanchez, M., Gonzalez-Garcia, M., Borras, C., Vina, J., Puertas, M.J., Sastre, J., Barja, G., 2010. Mitochondrial DNA sequences are present inside nuclear DNA in rat liver and increase with age. Mitochondrion 10 (5), 479–486.
Dunn, P.P., Stephens, P.J., Shirley, M.W., 1998. *Eimeria tenella*: two species of extrachromosomal DNA revealed by pulsed-field gel electrophoresis. Parasitol. Res. 84 (4), 272–275.
Feagin, J.E., 1992. The 6-kb element of *Plasmodium falciparum* encodes mitochondrial cytochrome genes. Mol. Biochem. Parasitol. 52 (1), 145–148.
Feagin, J.E., Mericle, B.L., Werner, E., Morris, M., 1997. Identification of additional rRNA fragments encoded by the *Plasmodium falciparum* 6 kb element. Nucleic Acids Res. 25 (2), 438–446.
Felsenstein, J., Churchill, G.A., 1996. A Hidden Markov Model approach to variation among sites in rate of evolution. Mol. Biol. Evol. 13 (1), 93–104.
Freyhult, E.K., Bollback, J.P., Gardner, P.P., 2007. Exploring genomic dark matter: a critical assessment of the performance of homology search methods on noncoding RNA. Genome Res. 17 (1), 117–125.
Gray, M.W., Lang, B.F., Burger, G., 2004. Mitochondria of protists. Annu. Rev. Genet. 38, 477–524.
Hamada, M., Kiryu, H., Sato, K., Mituyama, T., Asai, K., 2009. Prediction of RNA secondary structure using generalized centroid estimators. Bioinformatics 25 (4), 465–473.
Hausmann, K., Hülsmann, N., 1996. Protozoology, 2nd Edition. Georg Thieme Pub.
Hazkani-Covo, E., Zeller, R.M., Martin, W., 2010. Molecular poltergeists: mitochondrial DNA copies (numts) in sequenced nuclear genomes. PLoS Genet. 6 (2), e1000834.
Hikosaka, K., Watanabe, Y., Tsuji, N., Kita, K., Kishine, H., Arisue, N., Palacpac, N.M., Kawazu, S., Sawai, H., Horii, T., Igarashi, I., Tanabe, K., 2010. Divergence of the mitochondrial genome structure in the apicomplexan parasites, Babesia and Theileria. Mol. Biol. Evol. 27 (5), 1107–1116.
Janouskovec, J., Horak, A., Obornik, M., Lukes, J., Keeling, P.J., 2010. A common red algal origin of the apicomplexan, dinoflagellate, and heterokont plastids. Proc. Natl Acad. Sci. USA 107 (24), 10949–10954.
Jeurissen, S.H., Janse, E.M., Vermeulen, A.N., Vervelde, L., 1996. *Eimeria tenella* infections in chickens: aspects of host–parasite: interaction. Vet. Immunol. Immunopathol. 54 (1–4), 231–238.
Jones, D.T., Taylor, W.R., Thornton, J.M., 1992. The rapid generation of mutation data matrices from protein sequences. Comput. Appl. Biosci. 8 (3), 275–282.
Kairo, A., Fairlamb, A.H., Gobright, E., Nene, V., 1994. A 7.1 kb linear DNA molecule of *Theileria parva* has scrambled rDNA sequences and open reading frames for mitochondrially encoded proteins. EMBO J. 13 (4), 898–905.
Kishino, H., Hasegawa, M., 1989. Evaluation of the maximum likelihood estimate of the evolutionary tree topologies from DNA sequence data, and the branching order in hominoidea. J. Mol. Evol. 29 (2), 170–179.
Kuo, C.H., Wares, J.P., Kissinger, J.C., 2008. The Apicomplexan whole-genome phylogeny: an analysis of incongruence among gene trees. Mol. Biol. Evol. 25 (12), 2689–2698.
Lau, A.O., 2009. An overview of the *Babesia*, *Plasmodium* and *Theileria* genomes: a comparative perspective. Mol. Biochem. Parasitol. 164 (1), 1–8.
Levine, N.D., 1988. Progress in taxonomy of the Apicomplexan protozoa. J. Protozool. 35 (4), 518–520.
Mogi, T., Kita, K., 2010. Diversity in mitochondrial metabolic pathways in parasitic protists *Plasmodium* and *Cryptosporidium*. Parasitol. Int. 59 (3), 305–312.
Morrison, D.A., Ellis, J.T., 1997. Effects of nucleotide sequence alignment on phylogeny estimation: a case study of 18S rDNAs of apicomplexa. Mol. Biol. Evol. 14 (4), 428–441.
Nakai, Y., Edamura, K., Kanazawa, K., Shimizu, S., Hirota, Y., Ogimoto, K., 1993. Susceptibility to *Eimeria tenella* of chickens and chicken embryos of partly inbred lines possessing homozygous major histocompatibility complex haplotypes. Avian Dis. 37 (4), 1113–1116.
Nosek, J., Tomaska, L., 2003. Mitochondrial genome diversity: evolution of the molecular architecture and replication strategy. Curr. Genet. 44 (2), 73–84.
Ossorio, P.N., Sibley, L.D., Boothroyd, J.C., 1991. Mitochondrial-like DNA sequences flanked by direct and inverted repeats in the nuclear genome of *Toxoplasma gondii*. J. Mol. Biol. 222 (3), 525–536.
Palmer, J.D., Soltis, D., Soltis, P., 1992. Large size and complex structure of mitochondrial DNA in two nonflowering land plants. Curr. Genet. 21 (2), 125–129.

Perkins, S.L., 2008. Molecular systematics of the three mitochondrial protein-coding genes of malaria parasites: corroborative and new evidence for the origins of human malaria. Mitochondrial DNA 19 (6), 471–478.
Philippe, H., Snell, E.A., Bapteste, E., Lopez, P., Holland, P.W., Casane, D., 2004. Phylogenomics of eukaryotes: impact of missing data on large alignments. Mol. Biol. Evol. 21 (9), 1740–1752.
Preiser, P.R., Wilson, R.J., Moore, P.W., McCready, S., Hajibagheri, M.A., Blight, K.J., Strath, M., Williamson, D.H., 1996. Recombination associated with replication of malarial mitochondrial DNA. EMBO J. 15 (3), 684–693.
Richly, E., Leister, D., 2004. NUMTs in sequenced eukaryotic genomes. Mol. Biol. Evol. 21 (6), 1081–1084.
Shimodaira, H., 2002. An approximately unbiased test of phylogenetic tree selection. Syst. Biol. 51 (3), 492–508.
Shimodaira, H., Hasegawa, M., 1999. Multiple comparisons of log-likelihoods with applications to phylogenetic inference. Mol. Biol. Evol. 16 (8), 1114–1116.
Shirley, M.W., Ivens, A., Gruber, A., Madeira, A.M., Wan, K.L., Dear, P.H., Tomley, F.M., 2004. The *Eimeria* genome projects: a sequence of events. Trends Parasitol. 20 (5), 199–201.
Swofford, D.L., 2002. PAUP*. Phylogenetic analysis using parsimony (and other methods). Sinauer Associates, Sunderland, MA.
Thompson, J.D., Higgins, D.G., Gibson, T.J., 1994. CLUSTAL W: improving the sensitivity of progressive multiple sequence alignment through sequence weighting, position-specific gap penalties and weight matrix choice. Nucleic Acids Res. 22 (22), 4673–4680.
Ward, B.L., Anderson, R.S., Bendich, A.J., 1981. The mitochondrial genome is large and variable in a family of plants (cucurbitaceae). Cell 25 (3), 793–803.
Yang, Z., 2007. PAML 4: phylogenetic analysis by maximum likelihood. Mol. Biol. Evol. 24 (8), 1586–1591.

Parasitology International 60 (2011) 175–180

Contents lists available at ScienceDirect

Parasitology International

journal homepage: www.elsevier.com/locate/parint

Highly conserved gene arrangement of the mitochondrial genomes of 23 *Plasmodium* species

Kenji Hikosaka [a], Yoh-ichi Watanabe [b], Fumie Kobayashi [c], Seiji Waki [d], Kiyoshi Kita [b], Kazuyuki Tanabe [a,*]

[a] Laboratory of Malariology, International Research Center of Infectious Diseases, Research Institute for Microbial Diseases, Osaka University, Suita, Osaka, Japan
[b] Department of Biomedical Chemistry, Graduate School of Medicine, The University of Tokyo, Bunkyo-ku, Tokyo, Japan
[c] Department of Infectious Diseases, Faculty of Medicine, Kyorin University, Mitaka, Tokyo, Japan
[d] Gunma Prefectural College of Health Sciences, Maebashi, Gunma, Japan

ARTICLE INFO

Article history:
Received 22 November 2010
Received in revised form 25 January 2011
Accepted 7 February 2011
Available online 15 February 2011

Keywords:
Mitochondrion
Plasmodium
Apicomplexa
Genome structure
Inverted repeat sequence
Evolution

ABSTRACT

Mitochondrial (mt) genomes from diverse phylogenetic groups vary considerably in size, structure and organization. The genus *Plasmodium*, the causative agent of malaria, has the smallest mt genome in the form of a tandemly repeated, linear element of 6 kb. The *Plasmodium* mt genome encodes only three protein genes (*cox1*, *cox3* and *cob*) and large- and small-subunit ribosomal RNA (rRNA) genes, which are highly fragmented with 19 identified rRNA pieces. The complete mt genome sequences of 21 *Plasmodium* species have been published but a thorough investigation of the arrangement of rRNA gene fragments has been undertaken for only *Plasmodium falciparum*, the human malaria parasite. In this study, we determined the arrangement of mt rRNA gene fragments in 23 *Plasmodium* species, including two newly determined mt genome sequences from *P. gallinaceum* and *P. vinckei vinckei*, as well as *Leucocytozoon caulleryi*, an outgroup of *Plasmodium*. Comparative analysis reveals complete conservation of the arrangement of rRNA gene fragments in the mt genomes of all the 23 *Plasmodium* species and *L. caulleryi*. Surveys for a new rRNA gene fragment using hidden Markov models enriched with recent mt genome sequences led us to suggest the mtR-26 sequence as a novel candidate LSU rRNA fragment in the mt genomes of the 24 species. Additionally, we found 22–25 bp-inverted repeat sequences, which may be involved in the generation of lineage-specific mt genome arrangements after divergence from a common ancestor of the genera *Eimeria* and *Plasmodium/Leucocytozoon*.

1. Introduction

Mitochondria are essential organelles required for energy transduction and cellular functions, and are ubiquitous in almost all eukaryotic cells. Like nuclear genomes, mitochondrial (mt) genomes exhibit remarkable variation in structure and size [1]. The largest mt genome is found in land plants, in which the size ranges from 180 to 2400 kb [2,3]. The smallest mt genome is 6 kb and is found in the genus *Plasmodium*, the causal agent of malaria, which belongs to the phylum Apicomplexa. Almost all members of the Apicomplexa are clinically and/or economically important pathogenic parasites [4]. The mt genomes of apicomplexan parasites are highly diverse in structure and organization. In *Plasmodium*, the mt genome at the asexual erythrocytic stages is a tandemly repeated linear 6-kb element [5]. The 6-kb element contains only three protein-coding genes (cytochrome *c* oxidase subunit I [*cox1*] and III [*cox3*] and cytochrome *b* [*cob*]) and large subunit (LSU) and small subunit (SSU) ribosomal RNA (rRNA) genes. The two rRNA genes are highly fragmented with 19 identified rRNA sequences [6]. In *Babesia* and *Theileria*, genera that are closely related to *Plasmodium* [7], the mt genomes are monomeric linear, with sizes ranging from 6.6 kb to 8.2 kb, and contain terminal inverted repeats on both ends [8,9]. Although the *Babesia/Theileria* mt genomes encode the same three protein-coding genes as *Plasmodium*, gene arrangements and transcriptional direction are different from *Plasmodium*. Furthermore, only six fragmented LSU rRNA sequences have been identified in the *Babesia/Theileria* mt genomes, and the pattern of fragmentation differs drastically from *Plasmodium* [9]. Thus, the mt genomes of *Plasmodium* and *Babesia/Theileria* are structurally highly divergent.

We have recently shown that the mt genome of *Eimeria tenella*, which is distantly related to *Plasmodium* and *Babesia/Theileria*, has a concatemeric form and contains the same three protein-coding genes and 19 rRNA gene fragments as *Plasmodium*. This suggests that a concatemeric structure is an ancestral form of *Plasmdoium* and *Eimeria* mt genomes [10]. In spite of this similarity, the gene arrangements and transcriptional direction greatly differ between the *Plasmodium* and *Eimeria* mt genomes. It remains unknown how these differences were generated. Furthermore, even though the complete mt genome sequences are available for 21 *Plasmodium* species, little is known

* Corresponding author at: Laboratory of Malariology, International Research Center of Infectious Diseases, Research Institute for Microbial Diseases, Osaka University, 3-1 Yamadaoka, Suita, Osaka 565-0871, Japan. Tel.: +81 6 6879 4260; fax: +81 6 6879 4262.
E-mail address: kztanabe@biken.osaka-u.ac.jp (K. Tanabe).

1383-5769/$ – see front matter © 2011 Elsevier Ireland Ltd. All rights reserved.
doi:10.1016/j.parint.2011.02.001

about the variation in arrangement of the mt rRNA gene fragments. In this study, we report the arrangement of mt rRNA gene fragments in 23 *Plasmodium* species, including two newly determined mt genome sequences from *P. gallinaceum* and *P. vinckei vinckei*, as well as *Leucocytozoon caulleryi*, an outgroup of *Plasmodium*. There is complete conservation of the arrangement of rRNA gene fragments in the mt genomes of all the *Plasmodium* species and *L. caulleryi*. A novel candidate LSU rRNA fragment was found in the mt genomes of the parasite species. Additionally, 22- to 25-bp inverted repeat sequences were detected, which may be involved in the generation of lineage-specific mt genome arrangements.

2. Materials and methods

2.1. DNA sequencing

Genomic DNA of *P. gallinaceum* (A8 strain) was kindly provided by the late M. Shahabuddin (NIAID/NIH, USA). Genomic DNA of *P. vinckei vinckei* was extracted using a QIAamp DNA Blood Mini Kit (QIAGEN, Hilden, Germany) as previously described [11]. Nucleotide sequences of *P. gallinaceum* and *P. vinckei vinckei* mt genomes were determined by direct sequencing of polymerase chain reaction (PCR) products using conserved primers (Supplementary Table 1), which were designed by aligning the mt genome sequences of *P. falciparum* (DDBJ/EMBL/GenBank accession number M76611), *P. chabaudi* (AB379663), *P. relictum* (AY733089) and *P. mexicanum* (AB375765). The PCR amplification conditions, product purification and DNA sequencing protocol were the same as previously described [11]. Sequencing primers were designed to cover target regions in both directions. DNA sequencing was conducted on a 3130 Genetyx Analyzer automated sequencer (Applied Biosystems, Foster City, CA, USA) and was with at least two independent amplification products and sequencing runs. The sequences obtained in this study have been deposited in DDBJ/EMBL/GenBank with the following accession numbers: AB599930 (*P. gallinaceum* mt genome) and AB599931 (*P. vinckei vinckei* mt genome).

2.2. Gene annotation

Nucleotide sequences of the mt genomes from *P. gallinaceum* and *P. vinckei vinckei* and their deduced amino acid sequences were aligned with the mt genome sequences of *P. falciparum* (M76611) and other 20 *Plasmodium* species plus *L. caulleryi* retrieved from GenBank (Table 1) using ClustalW [12] with manual corrections. Protein-coding genes were predicted using previously annotated sequences from *P. falciparum*.

Putative rRNA gene fragments were identified using the annotated rRNA gene fragments from *P. falciparum* (M76611) as a query sequence [6] under suggested algorithm parameters [13] in NCBI BLAST 2.2 [14]. The termini of candidate gene fragments were determined using aligned sequences. The accession numbers of mt genomes used for identifying rRNA gene fragments are shown in Table 1.

Hidden Markov model of bacterial rRNA has recently been suggested to be useful to search for fragmented rRNA genes in metagenomic data [15]. In addition, the alpha-proteobacterial origin of mitochondria is widely accepted [16], and mt and bacterial rRNAs are closely related. We thus applied this model to identify novel rRNA gene fragments in *P. falciparum*. We also performed BLAST searches using *Tetrahymena pyriformis* mt rRNA fragments (AF160864). *T. pyriformis*, a member of ciliates, is closely related to the phylum Apicomplexa [17], and its mt rRNAs are fragmented [18,19]. Putative regions, missing from the *P. falciparum* mt rRNA, were surveyed with possible consensus sequence/structure from mt rRNAs [20] using scan_for_matches [21]. In addition, hidden Markov models constructed using mt sequences from *Babesia gibsoni* (AB499087), *Theileria orientalis* (AB499090) and *Theileria equi* (AB499091) [9] with HMMER 1.8.3 [22] were used to survey for mt genomes from representative *Plasmodium/Leucocytozoon* species (*P. falciparum*, *P. fragile*, and *L. caulleryi*).

2.3. Search for direct and inverted repeat sequences

Repeat sequences, such as an inverted repeat sequence, can potentially form secondary structures and may be involved in rearrangement events of genomes. Therefore, searches for repeat sequences were performed on the mt genomes for the 24 species used in this study (Table 1) and *E. tenella* (AB564272), which contains the same three protein-coding genes and 19 rRNA gene fragments as *Plasmodium* [10]. These searches were performed using the program REPFIND (http://zlab.bu.edu/repfind/) [23] under cut-off conditions of >10 nucleotides and a *P*-value<0.0001. Inverted repeat sequences were searched for using a 'self against self' BLASTN search [24] under cut-off conditions of >10 nucleotides. Furthermore, additional searches for repeats and

Table 1
Twenty three *Plasmodium* species and one *Leucocytozoon* species used in this study.

Species	Strain	Host	Accession number
Plasmodium gallinaceum	A8 strain	Bird	AB599930 (this study)
Plasmoidum vinckei vinckei	–	Rodent	AB599931 (this study)
Plasmodium falciparum	C10 line	Human	M76611
Plasmodium vivax	Salvador I	Human	NC_007243
Plasmodium malariae	Uganda I	Human	AB354570
Plasmodium ovale	Nigeria II	Human	AB354571
Plasmodium reichenowi	CDC1	Chimpanzee	NC_002235
Plasmodium hylobati	WAK (ATCC30194)	Gibbon	AB354573
Plasmodium cynomolgi	Langur	Monkey	AB434919
Plasmodium simiovale	(ATCC 30140)	Monkey	AB434920
Plasmodium fieldi	N-3 strain (ATCC30163)	Monkey	AB354574
Plasmodium inui	IM-Perak (ATCC30156)	Monkey	AB354572
Plasmodium fragile	Hackeri	Monkey	AY722799
Plasmodium coatneyi	CDC strain	Monkey	AB354575
Plasmodium knowlesi	Malayan strain (ATCC30192)	Monkey/Human	NC_007232
Plasmodium gonderi	(ATCC 30045)	Monkey	AB434918
Plasmodium yoelii	17XNL	Rodent	MALPY00209
Plasmodium chabaudi	AS strain	Rodent	AB379663
Plasmodium berghei	ANKA strain	Rodent	ANKA contig 5406
Plasmodium relictum	(ATCC 30141)	Bird	AY733089
Plasmodium juxtanucleare	–	Bird	AB250415
Plasmodium mexicanum	–	Lizard	AB375765
Plasmodium floridense	–	Lizard	NC_009961
Leucocytozoon caulleryi	–	Bird	AB302215

inverted repeats were performed using GENETYX software (Version 8; SDC, Tokyo, Japan).

3. Results

3.1. Mitochondrial genome organization of P. gallinaceum and P. vinckei vinckei

We sequenced the mt genomes from *P. gallinaceum* (6.0 kb) and *P. vinckei vinckei* (5.9 kb), and identified three protein-coding genes (Fig. 1A and B). These genes are syntenic to the *P. falciparum* mt genome (Fig. 1C).

Using the *P. falciparum* mt genome sequence as a query, we also identified 12 fragments of LSU rRNA gene and seven fragments of SSU rRNA gene in the mt genomes of *P. gallinaceum*, *P. vinckei vinckei*, and 20 other *Plasmodium* species and *L. caulleryi* (Supplementary Table 2). Several approaches were undertaken to explore putative missing sequences of *Plasmodium* mt rRNA gene fragments. Searches with bacterial rRNA hidden Markov models and BLAST searches with *T. pyriformis* mt rRNA sequences both failed to detect any additional fragmented rRNA candidates. Additional searches using hidden Markov models constructed with *Babesia/Theileria* sequences revealed that six nucleotides in mtR-26, a recently identified *P. falciparum* transcript [25], are complementary to a region in RNA1, one of the mt LSU rRNA fragments of *P. falciparum*, if G–U pairs are allowed (Fig. 2A). G–U "wobble" base pairing is one of the most frequently found "mismatches" in various RNAs including rRNAs [26]. Thus, the interaction between RNA1 and mtR-26 including G–U pair(s) seems to be very likely. The mtR-26 corresponds to *E. coli* LSU rRNA positions between 579–584 and flanking regions, and is perfectly conserved in the mt genomes of the 23 *Plasmodium* species and *L. caulleryi* (Fig. 2B) (Supplementary Table 2). Thus, we suggest that *P. falciparum* mtR-26 and its putative homologs in 22 *Plasmodium* species (as well as *L. caulleryi*) are a fragmented LSU rRNA. The organization and predicted transcriptional direction of rRNA gene fragments including mtR-26 are completely conserved among the 24 parasite species examined here.

3.2. Comparison of mt genome sequences

Pairwise sequence identity of *cox3*, *cox1* and *cob* is comparable among the 23 *Plasmodium* species and *L. caulleryi* (Table 2): 79.9–98.9% for *cox3*, 85.0–99.2% for *cox1* and 82.5–99% for *cob* at the nucleotide sequence level, and 79.6–99.6% for COX3, 90.6–100% for COX1 and 82.2–100% for COB at the amino acid sequence level. In contrast to these protein-coding genes, pairwise sequence identity of 20 rRNA gene fragments is very high, 94.4–99.9% (94.7–100% for 13 LSUs and 93.8–100% for seven SSUs) among the 24 species. Pairwise sequence identity of intergenic regions is also high, 89.5–99.4% among the 24 species. Pairwise sequence identity of 10 representative parasites is given in Supplementary Tables 3–5.

Small differences in size of the 24 mt genomes (5948 bp of *P. vinckei vinckei* to 6014 bp of *P. juxtanucleare*) are due to variations in the number of A or T homopolymers, and insertion/deletion of A or T in rRNA gene fragments and intergenic regions.

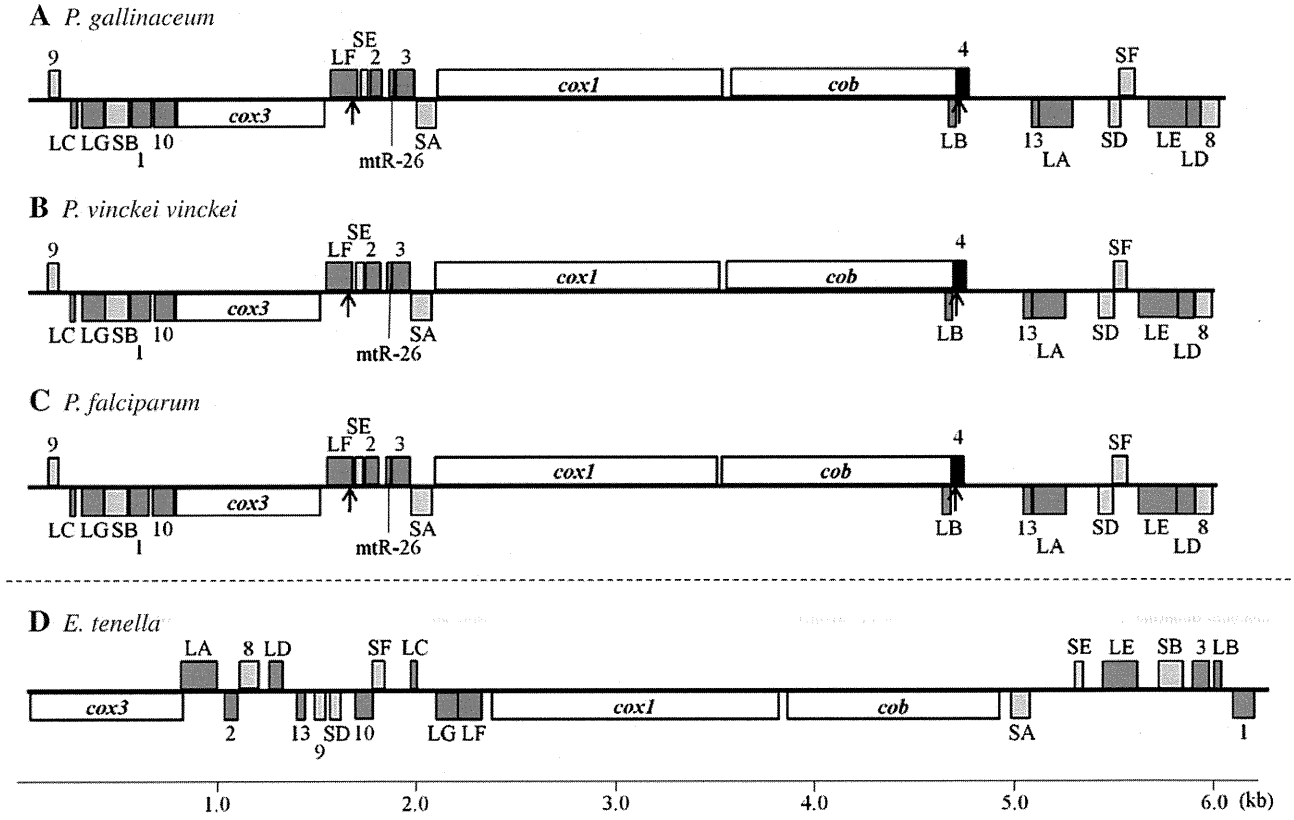

Fig. 1. Structure of the mitochondrial (mt) genomes of *P. gallinaceum* (A) and *P. vinckei vinckei* (B). Shown for comparison are the mt genomes of *P. falciparum* (C) (M76611) and *Eimeria tenella* (D) (AB564272). Elements within these genomes are tandemly repeated, so the designation of both termini is arbitrary. Genes shown above the bold line in each genome are transcribed left to right and those below are transcribed from right to left. Dark and light grey boxes indicate fragments of LSU and SSU rRNA genes, respectively. Black boxes indicate transcript, RNA4, which has not been annotated (M76611). Arrows indicate the position of inverted repeat sequences. *cox1*, cytochrome *c* oxidase subunit I; *cox3*, cytochrome *c* oxidase subunit III; *cob*, cytochrome *b*.

A

RNA1 5' G C U G A C 3'
. * . . * *
mtR-26 3' U G G U U G 5'

B

P. falciparum mtR-26	T G T T A T G T T G T T G G T T T A A G C C C
P. gallinaceum	• • • • • • • C • • • • • • • • • • • • • • • •
P. vinckei vinckei	• •
P. vivax	• •
P. malariae	• •
P. ovale	• •
P. reichenowi	• •
P. hylobati	• •
P. cynomolgi	• •
P. simiovale	• •
P. fieldi	• •
P. inui	• •
P. fragile	• •
P. coatneyi	• •
P. knowlesi	• A •
P. gonderi	• •
P. yoelii	• •
P. chabaudi	• •
P. berghei	• •
P. relictum	• • • • • • • C • • • • • • • • • • • • • • • •
P. juxtanucleare	• • • • • • • C • • • • • • • • • • • • • • • •
P. mexicanum	• • • • • • • C • • • • • • • • • • • • • • • •
P. floridense	• • • • • • • C • • • • • • • • • • • • • • • •
L. caulleryi	• • • • • • • C • • • • • • • • • • • • • • • •

Fig. 2. Complementarity between *P. falciparum* mtR-26 and RNA1 (A), and nucleotide sequence alignments of *P. falciparum* mtR-26 and its homologs from 22 *Plasmodium* species and *Leucocytozoon caulleryi* (B). In panel A, the six nucleotides of mtR-26 correspond to *E. coli* LSU rRNA positions between 579 and 584. Dots and asterisks indicate G–U base pairing motifs and A–U/G–C pairs, respectively. In panel B, a predicted sequence region complementary to RNA1 is boxed. Dots indicate identical nucleotides to *P. falciparum* mtR-26.

3.3. Repeat sequences of the Plasmodium mt genomes

Searches for direct repeat sequences identified one to six repeats with lengths of 10 to 15 bp in the mt genomes of all species examined here, except *P. gallinaceum* and *P. floridense*. These repeat sequences are not conserved among the 23 species but one pair of inverted repeat sequences of 22 to 25 bp is conserved in all *Plasmodium* species and *L. caulleryi* (Fig. 3). These inverted repeat sequences were located at the 3′ region of LSUF, which has been identified as a LSU rRNA gene fragment and at the 5′ region of RNA4, the function of which in the *P. falciparum* mt genome (M76611) is unknown (Feagin, personal communication). The nucleotide positions of RNA4 in each species examined here are shown in Supplementary Table 2. In contrast, no inverted repeat sequences were found in the *E. tenella* mt genome.

4. Discussion

This study shows that the organization and predicted transcriptional direction of mt protein-coding genes and mt rRNA gene fragments are highly conserved among the 23 *Plasmodium* species and *L. caulleryi* examined. In addition, arrangements and nucleotide sequences of intergenic regions ranging from 953 bp to 1011 bp, which represent approximately one-sixth of the 6-kb genome, are also highly conserved. Recently, transcription of almost all intergenic regions of *P. falciparum* mt genome has been demonstrated [25]. These highly conserved sequence regions may thus code for functional RNAs. This study suggests that one of the transcripts, mtR-26, is a fragment of the LSU rRNA gene.

The high degree of conservation of the *Plasmodium* mt genome structure may be due to structural constraints on the genome. In general, mt genomes display a tendency of size reduction or deletional bias [27]. Since the *Plasmodium* mt genome is the smallest so far known, a further reduction and rearrangement of sequences may deleteriously affect the function of their genomes. Consistent with this proposition, the size and gene arrangement of vertebrate mt genomes remain virtually unchanged over long evolutionary time; e.g. the gene arrangements of human and trout mt genomes are nearly identical [28]. Although vertebrate mt genomes are much larger (16 kb) than the *Plasmodium* mt genome, the high conservation of vertebrate mt genome structures supports our proposition that structural constraints limit mt genome change.

In the present study, an inverted repeat sequence was identified in all *Plasmodium* species and *L. caulleryi*. The presence of this inverted repeat sequence allows us to infer a scenario for the evolutionary trajectory of the mt genome structures of *Plasmodium* and *E. tenella*. A comparison of the arrangements of three protein coding genes between *Plasmodium* and *Eimeria* suggests that at least one inversion event of a region containing *cox1/cob* or *cox3* must have occurred in an ancestral lineage leading to either *Plasmodium* or *Eimeria*. The inverted repeat sequences are located 5′ to *cox1* and 3′ to *cob*. Therefore, these inverted repeats may have been involved in an inversion event of either *cox1/cob* or *cox3* in an ancestral lineage. The present data set does not predict whether the inverted repeats were inserted into an ancestral lineage of *Plasmodium* or deleted from an ancestral lineage of *Eimeria*.

Table 2
Sequence identity of protein-coding genes, rRNA gene fragments and the intergenic region of the mitochondrial genomes of 23 *Plasmodium* species and *Leucocytozoon caulleryi*.

Region		No. of sites	Sequence identity	
			Mean ± SE[a] (%)	Range (%)
Protein-coding gene	*cox3* + *cox1* + *cob*	3318 nt	89.4 ± 0.35	83.0–98.9
	(Amino acid sequence)	(1106 aa)	(92.0 ± 0.47)	(85.6–99.5)
	cox3	753 nt	88.0 ± 0.61	79.9–98.9
	(Amino acid sequence)	(251 aa)	(88.4 ± 1.14)	(79.6–99.6)
	cox1	1434 nt	89.6 ± 0.42	85.0–99.2
	(Amino acid sequence)	(478 aa)	(94.7 ± 0.61)	(90.6–100)
	Cob	1131 nt	89.9 ± 0.45	82.5–99.0
	(Amino acid sequence)	(377 aa)	(91.0 ± 0.85)	(82.2–100)
rRNA gene fragment	LSU + SSU	1624 nt	97.8 ± 0.20	94.4–99.9
	LSU	1091 nt	97.7 ± 0.26	94.7–100
	SSU	533 nt	97.9 ± 0.30	93.8–100
Intergenic regions		884 nt	94.3 ± 0.39	89.5–99.4

[a] Standard error (SE) estimates were obtained by a bootstrap procedure (500 replicates) using MEGA4 [30].

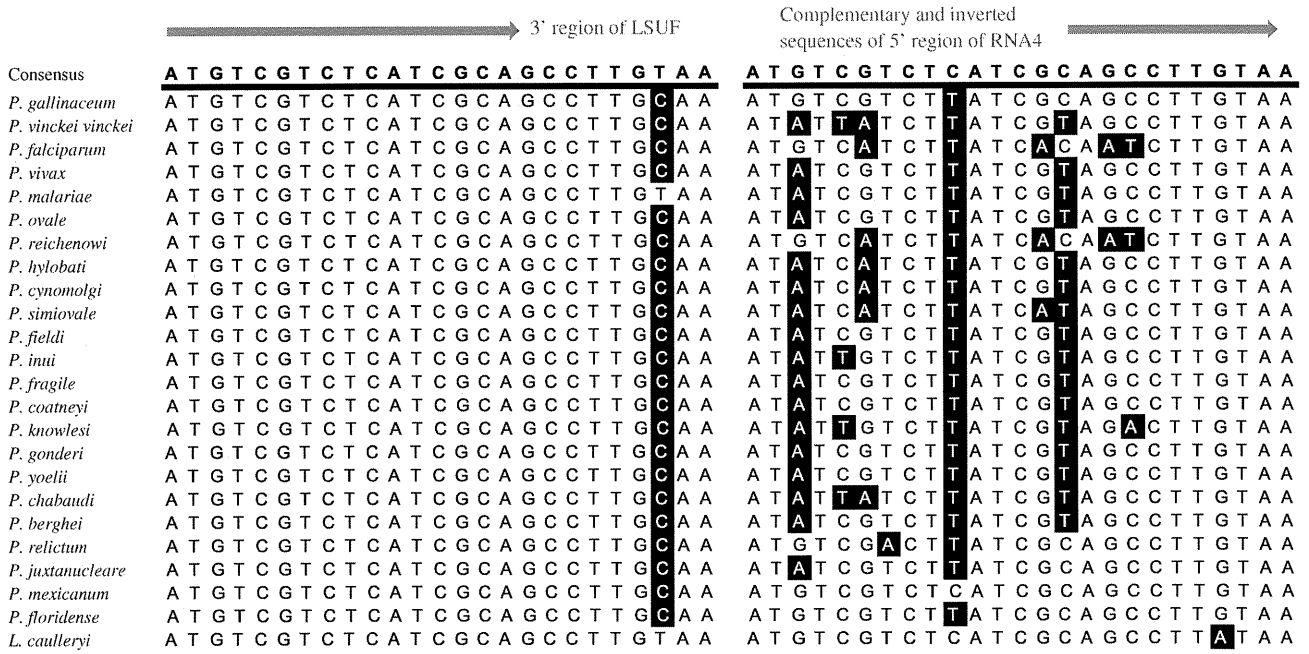

Fig. 3. Nucleotide sequence alignments of inverted repeats in the mt genomes of 23 *Plasmodium* species and *Luecocytozoon caulleryi*. Alignments are located at the 3′ region of LSUF (left) and 5′ region of RNA4 (right). RNA4 sequences shown are complementary and inverted. White characters highlighted in black indicate nucleotides differing from the consensus sequence.

A closer examination of the gene order of *cox1* and *cob*, as well as many of the 19 rRNA gene fragments, reveals that it is considerably different between *Plasmodium* and *Eimeria*. This difference cannot be explained by an inversion event. It is generally assumed that the duplication and random loss (TDRL) model [28] accounts for changes in gene order. According to the TDRL model, genes or gene fragments are duplicated and some of these are subsequently lost thereby generating a new gene order. For example, a duplication of a segment containing *cox1/cob* in the *Plasmodium* mt genome, followed by the loss of the 5′-end *cox1* and the 3′-end *cob*, can generate the gene order of *cob/cox1*, which is found in the *Eimeria* mt genome (shown in a complementary direction, in Fig. 1). However, rearrangements of rRNA gene fragments are very extensive between the mt genomes of *Plasmodium* and *Eimeria* (Fig. 1). Therefore, TDRL model may be too simple to adequately account for the observed rearrangements of rRNA gene fragments.

Complete mt genome sequences are now available for 23 *Plasmodium* species but the biological function of their very compact mt genome remains largely unknown [29]. It is extremely difficult to purify and therefore characterize mitochondria from *Plasmodium*. The high conservation of mt genomes among *Plasmodium* species may shed some light on the importance of mt function. Further molecular and biochemical studies are required to determine the significance of this sequence conservation.

Acknowledgements

This work was supported by Grant-in-Aids for Scientific Research from the Ministry of Education, Culture, Sports, Science and Technology of Japan (18073013) and from Japan Society for Promotion of Sciences (18GS03140013 and 20390120).

Appendix A. Supplementary data

Supplementary data to this article can be found online at doi:10.1016/j.parint.2011.02.001.

References

[1] Gray MW, Lang BF, Burger G. Mitochondria of protists. Annu Rev Genet 2004;38:477–524.
[2] Ward BL, Anderson RS, Bendich AJ. The mitochondrial genome is large and variable in a family of plants (cucurbitaceae). Cell 1981;25:793–803.
[3] Palmer JD, Soltis D, Soltis P. Large size and complex structure of mitochondrial DNA in two nonflowering land plants. Curr Genet 1992;21:125–9.
[4] Levine ND. Progress in taxonomy of the apicomplexan protozoa. J Protozool 1988;35:518–20.
[5] Wilson RJ, Williamson DH. Extrachromosomal DNA in the apicomplexa. Microbiol Mol Biol Rev 1997;61:1–16.
[6] Feagin JE, Mericle BL, Werner E, Morris M. Identification of additional rRNA fragments encoded by the *Plasmodium falciparum* 6 kb element. Nucleic Acids Res 1997;25:438–46.
[7] Lau AO. An overview of the *Babesia*, *Plasmodium* and *Theileria* genomes: a comparative perspective. Mol Biochem Parasitol 2009;164:1–8.
[8] Kairo A, Fairlamb AH, Gobright E, Nene V. A 7.1 kb linear DNA molecule of *Theileria parva* has scrambled rDNA sequences and open reading frames for mitochondrially encoded proteins. EMBO J 1994;13:898–905.
[9] Hikosaka K, Watanabe Y, Tsuji N, Kita K, Kishine H, Arisue N, et al. Divergence of the mitochondrial genome structure in the apicomplexan parasites, Babesia and Theileria. Mol Biol Evol 2010;27:1107–16.
[10] Hikosaka K, Nakai Y, Watanabe Y, Tachibana SI, Arisue N, Palacpac NM, et al. Concatenated mitochondrial DNA of the coccidian parasite *Eimeria tenella*. Mitochondrion 2011;11:273–8.
[11] Sakihama N, Mitamura T, Kaneko A, Horii T, Tanabe K. Long PCR amplification of *Plasmodium falciparum* DNA extracted from filter paper blots. Exp Parasitol 2001;97:50–4.
[12] Thompson JD, Higgins DG, Gibson TJ. CLUSTAL W: improving the sensitivity of progressive multiple sequence alignment through sequence weighting, position-specific gap penalties and weight matrix choice. Nucleic Acids Res 1994;22:4673–80.
[13] Freyhult EK, Bollback JP, Gardner PP. Exploring genomic dark matter: a critical assessment of the performance of homology search methods on noncoding RNA. Genome Res 2007;17:117–25.
[14] Altschul SF, Gish W, Miller W, Myers EW, Lipman DJ. Basic local alignment search tool. J Mol Biol 1990;215:403–10.
[15] Huang Y, Gilna P, Li W. Identification of ribosomal RNA genes in metagenomic fragments. Bioinformatics 2009;25:1338–40.
[16] Gray M, Spencer DF. Organellar Evolution. Evolution of microbial life, 54. Cambridge University Press; 1997. p. 109–26.
[17] Cavalier-Smith T. Kingdom protozoa and its 18 phyla. Microbiol Rev 1993;57:953–94.
[18] Schnare MN, Heinonen TY, Young PG, Gray MW. A discontinuous small subunit ribosomal RNA in *Tetrahymena pyriformis* mitochondria. J Biol Chem 1986;261:5187–93.

[19] Heinonen TY, Schnare MN, Young PG, Gray MW. Rearranged coding segments, separated by a transfer RNA gene, specify the two parts of a discontinuous large subunit ribosomal RNA in *Tetrahymena pyriformis* mitochondria. J Biol Chem 1987;262:2879–87.
[20] Cannone JJ, Subramanian S, Schnare MN, Collett JR, D'Souza LM, Du Y, et al. The comparative RNA web (CRW) site: an online database of comparative sequence and structure information for ribosomal, intron, and other RNAs. BMC Bioinform 2002;3:2.
[21] Dsouza M, Larsen N, Overbeek R. Searching for patterns in genomic data. Trends Genet 1997;13:497–8.
[22] Eddy SR. Profile hidden Markov models. Bioinformatics 1998;14:755–63.
[23] Betley JN, Frith MC, Graber JH, Choo S, Deshler JO. A ubiquitous and conserved signal for RNA localization in chordates. Curr Biol 2002;12:1756–61.
[24] Altschul SF, Madden TL, Schaffer AA, Zhang J, Zhang Z, Miller W, et al. Gapped BLAST and PSI-BLAST: a new generation of protein database search programs. Nucleic Acids Res 1997;25:3389–402.
[25] Raabe CA, Sanchez CP, Randau G, Robeck T, Skryabin BV, Chinni SV, et al. A global view of the nonprotein-coding transcriptome in *Plasmodium falciparum*. Nucleic Acids Res 2010;38:608–17.
[26] Gutell RR, Larsen N, Woese CR. Lessons from an evolving rRNA: 16S and 23S rRNA structures from a comparative perspective. Microb Rev 1994;58:10–26.
[27] Andersson SG, Kurland CG. Reductive evolution of resident genomes. Trends Microbiol 1998;6:263–8.
[28] Boore JL. Animal mitochondrial genomes. Nucleic Acids Res 1999;27:1767–80.
[29] Mogi T, Kita K. Diversity in mitochondrial pathways in parasitic protists *Plasmodium* and *Cryptosporidium*. Parasitol Int 2010;59:305–12.
[30] Tamura K, Dudley J, Nei M, Kumar S. MEGA4: Molecular Evolutionary Genetics Analysis (MEGA) software version 4.0. Mol Biol Evol 2007;24:1596–9.

Tetrahedron 67 (2011) 6582–6586

Contents lists available at ScienceDirect

Tetrahedron

journal homepage: www.elsevier.com/locate/tet

Ukulactones A and B, new NADH-fumarate reductase inhibitors produced by *Penicillium* sp. FKI-3389

Mihoko Mori [a,b], Hiromi Morimoto [c], Yong-Pil Kim [a], Hideaki Ui [a,b], Kenichi Nonaka [a], Rokuro Masuma [a,b], Kimitoshi Sakamoto [d], Kiyoshi Kita [d], Hiroshi Tomoda [c], Kazuro Shiomi [a,b,*], Satoshi Ōmura [a,*]

[a] *Kitasato Institute for Life Sciences, Kitasato University, 5-9-1 Shirokane, Minato-ku, Tokyo 108-8641, Japan*
[b] *Graduate School of Infection Control Sciences, Kitasato University, 5-9-1 Shirokane, Minato-ku, Tokyo 108-8641, Japan*
[c] *School of Pharmacy, Kitasato University, 5-9-1 Shirokane, Minato-ku, Tokyo 108-8641, Japan*
[d] *Graduate School of Medicine, The University of Tokyo, 7-3-1 Hongo, Bunkyo-ku, Tokyo 113-0033, Japan*

ARTICLE INFO

Article history:
Received 29 April 2011
Received in revised form 20 May 2011
Accepted 20 May 2011
Available online 27 May 2011

Keywords:
Electron transport enzyme inhibitor
NADH-fumarate reductase
Penicillium
Ukulactone

ABSTRACT

Screening for NADH-fumarate reductase inhibitors led to the isolation of the new polyketide compounds, ukulactones A and B (**1** and **2**, Fig. 1) from a culture broth of *Penicillium* sp. FKI-3389. The structure of ukulactone A was elucidated as a methylated derivative of prugosene A1, which was produced by *Penicillium rugulosum* and NOESY experiment revealed ukulactone B was a stereoisomer of ukulactone A. Ukulactone A showed potent inhibitory activity against NADH-fumarate reductase of the roundworm *Ascaris suum* in vitro.

1. Introduction

NADH-fumarate reductase (NFRD), consisting of mitochondrial complexes I and II, is an electron transport system involved in a unique energy metabolic pathway found in many anaerobic organisms, such as helminths.[1] This system is used to generate ATP in the absence of oxygen and allows helminths to live in anaerobic circumstances inside the host. Therefore, a selective inhibitor of NFRD is expected to be a good anthelmintic. We have screened for NFRD inhibitors in culture broths of fungi using helminth (*Ascaris suum*) mitochondria, and found some potent inhibitors, such as nafuredin,[2] atpenins,[3] verticipyrone,[4] and paecilaminol.[5] During this screening we obtained new NFRD inhibitors, ukulactones A and B (**1** and **2**, Fig. 1), from the culture broth of the terrestrial fungus *Penicillium* sp. FKI-3389. In this report, we describe the isolation, structural elucidation, and biological activities of these two ukulactones.

2. Results and discussion

2.1. Isolation and structure elucidation of ukulactones A (1) and B (2)

A solid culture of *Penicillium* sp. FKI-3389 was extracted with EtOAc and the extract was purified by silica gel column chromatography and HPLC. From 3 kg of the solid broth, 515 mg of **1** and 3.5 mg of **2** were isolated.

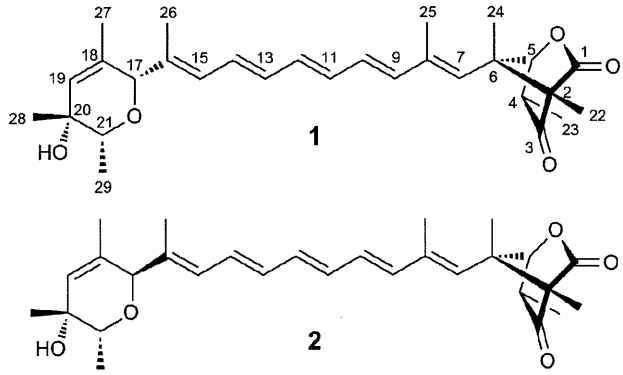

Fig. 1. Structures of ukulactones A (**1**) and B (**2**).

Ukulactone A (**1**) was obtained as a yellow syrup. The molecular formula was elucidated to be $C_{29}H_{38}O_5$ by HRFABMS (observed $[M]^+$ at 466.2722, calcd $[M]^+$ 466.2719). The characteristic absorption maxima at 325, 340, and 358 nm in the UV spectrum, strongly suggested that **1** has a pentaene in the structure. The IR absorptions indicated the presence of hydroxyl (3730 cm^{-1}) and carbonyl (1795 and 1745 cm^{-1}) groups.

* Corresponding authors. E-mail addresses: shiomi@lisci.kitasato-u.ac.jp (K. Shiomi), omuras@insti.kitasato-u.ac.jp (S. Ōmura).

0040-4020/$ – see front matter © 2011 Elsevier Ltd. All rights reserved.
doi:10.1016/j.tet.2011.05.090

Table 1
^{1}H and ^{13}C NMR data of **1** and **2** (in $CDCl_3$)

Position	**1**[a]		**2**[b]	
	δ_H (Int., mult., J in Hz)	δ_C mult.	δ_H (Int., mult., J in Hz)	δ_C mult.
1		171.4 s		171.4 s
2		70.1 s		70.1 s
3		207.6 s		207.6 s
4	2.65 (1H, qd, 7.4, 2.2)	44.3 d	2.66 (1H, qd, 7.4, 2.2)	44.3 d
5	5.15 (1H, d, 2.2)	85.2 d	5.16 (1H, d, 2.2)	85.2 d
6		57.9 s		57.9 s
7	5.21 (1H, s)	127.7 d	5.22 (1H, s)	127.8 d
8		138.8 s		138.8 s
9	6.12 (1H, d, 14.4)	136.1 d	6.13 (1H, d, 14.4)	136.2 d
10	6.32 (1H, dd, 14.4, 10.9)	133.5 d	6.38 (1H, dd, 14.4, 10.9)	134.2 d
11	6.27 (1H, dd, 14.4, 10.9)	132.7 d	6.24 (1H, dd, 14.4, 10.9)	132.8 d
12	6.37 (1H, dd, 14.4, 10.9)	134.3 d	6.31 (1H, dd, 14.4, 10.9)	133.6 d
13	6.30 (1H, dd, 14.4, 10.9)	129.5 d	6.28 (1H, dd, 14.4, 10.9)	129.5 d
14	6.47 (1H, dd, 14.4, 10.9)	129.1 d	6.49 (1H, dd, 14.4, 10.9)	129.2 d
15	6.16 (1H, d, 10.9)	130.5 d	5.82 (1H, d, 10.9)	128.9 d
16		136.3 s		134.9 s
17	4.36 (1H, s)	85.2 d	4.30 (1H, s)	80.7 d
18		136.3 s		134.8 s
19	5.68 (1H, s)	130.8 d	5.66 (1H, s)	130.1 d
20		67.0 s		67.3 s
21	3.47 (1H, q, 6.3)	77.2 d	3.51 (1H, q, 6.3)	71.0 d
22	1.21 (3H, s)	4.8 q	1.21 (3H, s)	4.8 q
23	1.18 (3H, d, 7.4)	11.6 q	1.19 (3H, d, 7.4)	11.6 q
24	1.40 (3H, s)	16.8 q	1.40 (3H, s)	16.8 q
25	1.89 (3H, s)	14.3 q	1.90 (3H, s)	14.4 q
26	1.70 (3H, s)	12.0 q	1.90 (3H, s)	16.2 q
27	1.47 (3H, s)	18.5 q	1.62 (3H, s)	20.1 q
28	1.14 (3H, s)	23.5 q	1.13 (3H, s)	23.7 q
29	1.22 (3H, d, 6.3)	14.2 q	1.15 (3H, d, 6.3)	14.0 q

[a] Recorded at 300 MHz (^{1}H) and 75 MHz (^{13}C).
[b] Recorded at 400 MHz (^{1}H) and 100 MHz (^{13}C).

The ^{1}H and ^{13}C NMR data of **1** are shown in Table 1. Analysis of the ^{1}H and ^{13}C NMR, DEPT, and HSQC spectra revealed the presence of eight methyl groups, one sp^3 methine carbon, three quaternary carbons, three oxymethine carbons, nine sp^2 methine carbons, three sp^2 quaternary carbons, one carboxyl group, and one carbonyl group. The COSY correlations showed the presence of a spin system of seven olefin protons (from H-9 to H-15) in a pentaene moiety suggested by UV spectrum. The configurations of the olefins were assigned to be *trans* by their coupling constants (J=14.4 and 10.9 Hz). In the pentaene moiety, NOE correlations between H-7 and H-9 and between H-14 and H-26 were observed (Fig. 2). In addition, ^{13}C chemical shifts of the olefin methyl carbons C-25 (δ 14.3) and C-26 (δ 12.0) suggested the configuration of the pentaene moiety was all-*trans*.[6]

HMBC correlations from methyl proton H-25 to C-7, C-8, and C-9 and from H-26 to C-15, C-16, and C-17 were observed (Figs. 3 and 5), thus two methyl moieties were attached to C-8 and C-16 of the pentaene substructure of **1**, respectively. By the HMBC correlations in Fig. 3, another partial structure was deduced to be 4,6,7-trimethyl-2-oxabicyclo[2.2.1]heptane-3,5-dione contained in shimalactones A and B,[7] prugosenes A1–A3,[8] coccidiostatin A[9] and wartmannilactones E, F, and H.[10] The ^{1}H and ^{13}C chemical shifts of this substructure were in good accordance with those of shimalactones A and B in $CDCl_3$.[7] The HMBC correlations from the methyl proton H-24 revealed that this bicyclo unit connected to C-7 of the pentaene (Fig. 3). We conducted a NOESY experiment to analyze relative configuration of the bicyclo unit. The observed NOE correlations are shown in Fig. 4. The data indicated the relative configuration of this unit was (2*S*,4*R*,5*S*,6*S*) the same as prugosenes A1–A3.[8]

HMBC correlations (Fig. 5) clarified **1** had the 3,6-dihydro-3-hydroxy-2,3,5-trimethyl-2*H*-pyran ring also contained in prugosene A1[8] and wortmannilactones E and F.[10] The relative conformation of the dihydropyran ring was (17*S*,20*R*,21*R*), indicated by NOE correlations from H-17 to H-21, H-26 and H-27, and those from H-28 to H-19 and H-21 (Fig. 6). Therefore, ukulactone A was deduced to be an 8-methyl derivative of prugosene A1.

Ukulactone B (**2**) was also obtained as a yellow syrup. The molecular formula was elucidated to be $C_{29}H_{38}O_5$, the same value as ukulactone A (**1**) by HRFABMS. UV and IR spectra were almost identical, but the sign of $[\alpha]_D$, which was opposite to that of **1**, suggested **2** is a stereoisomer of **1**. As compared with ^{1}H and ^{13}C

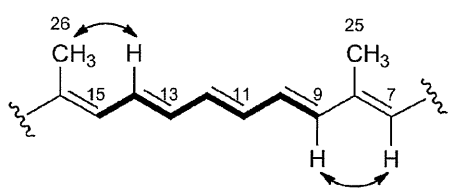

Fig. 2. COSY (bold line) and key NOESY (arrow) correlations of pentaene unit of **1**.

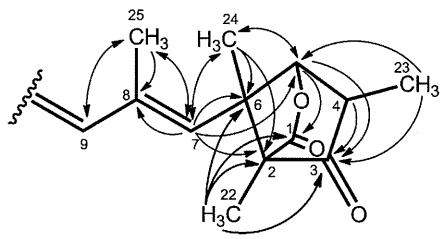

Fig. 3. HMBC correlations of the trimethyloxabicyclo[2.2.1]heptane unit of **1**.

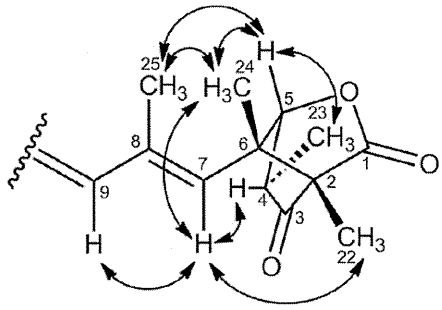

Fig. 4. NOESY correlations of the trimethyloxabicyclo[2.2.1]heptane unit of **1**.

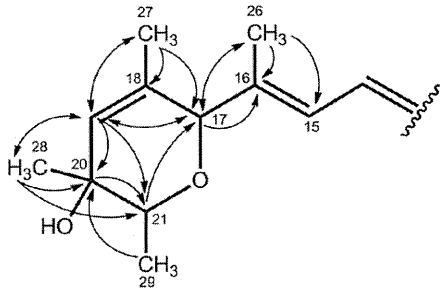

Fig. 5. HMBC correlations of the dihydropyran unit of **1**.

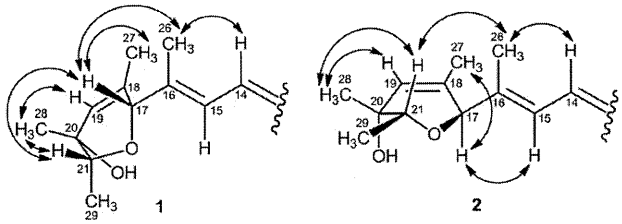

Fig. 6. NOESY correlations of the dihydropyran unit of **1** and **2**.

NMR spectra of **1**, the chemical shifts of signals assigned to the dihydropyran ring were changed from **1** (Table 1), although the HMBC correlations showed **1** and **2** had the same planar structure. These results suggested **2** had a different configuration in the dihydropyran ring moiety compared with **1**. This was elucidated by a NOESY experiment. The NOEs observed in the dihydropyran ring of **2** are shown in Fig. 6. Compared with the data of **1**, the NOE correlation between H-17 and H-21 is not observed and the correlation between H-15 and H-17 was only observed in **2**. Therefore, the relative configuration was defined as (17*R*,20*R*,21*R*). We also confirmed the 2-oxabicyclo[2.2.1]heptane unit had the same configuration (2*S*,4*R*,5*S*,6*S*) as that of **1** by analysis of NOESY data. From the above data **2** was elucidated to be the C-17 epimer (17*R*-epimer) of **1**. While the difference between two compounds was only the conformation of C-17, **2** was much more labile than **1**.

3. Biological activities

Inhibitory activities of **1** and **2** against electron transport system enzymes were evaluated using submitochondrial particles of *A. suum* and bovine heart (Table 2). Compound **1** inhibited NADH-fumarate reductase (NFRD, composed of complexes I and II) from *A. suum* with an IC_{50} value of 2.4 nM, although the inhibition against mammal enzymes NADH oxidase (constituted with complexes I, III, and IV) and succinate-cytochrome *c* reductase (constituted of complexes II and III) from bovine heart was weak, with IC_{50} values of 9000 nM and 68,000 nM, respectively. Next we examined the selectivity of inhibitory activity of **1** against each complex. Compound **1** inhibited NADH-rhodoquinone reductase (complex I) activity with an IC_{50} value of 55 nM, but it did not affect rhodoquinol-fumarate reductase (complex II) activity at 100 μM. On the other hand, **1** showed only weak inhibitory activities against each complex of bovine heart. Therefore **1** is concluded to be a selective inhibitor of helminth complex I, similar to nafuredin.[2a]

Table 2
Inhibition of electron transport enzymes by **1** and **2**

	Enzyme	Complex	IC_{50} (nM)	
			1	**2**
A. suum	NADH-fumarate reductase	I+II	2.4	470
	NADH-rhodoquinone reductase	I	55	NT
	Rhodoquinol-fumarate reductase	II	>100,000	NT
Bovine heart	NADH oxidase	I+III+IV	9000	16,000
	Succinate-cytochrome *c* reductase	II+III	68,000	30,000
	NADH-ubiquinone reductase	I	28,000	NT
	Succinate-ubiquinone reductase	II	>100,000	NT
	Ubiquinol-cytochrome *c* reductase	III	32,000	NT

NT: not tested.

The IC_{50} value of the epimer **2** against NFRD was 470 nM, about 200 times weaker than **1**. However **2** inhibited NADH oxidase and succinate-cytochrome *c* reductase at the IC_{50} values of 16,000 nM and 30,000 nM, respectively, which were similar to those of **1**. These data suggested **1** had more helminth specific-NFRD inhibitory activity compared to **2**. The specificity might be due to the conformation of the dihydropyran ring, which would be considerably changed by altering the configuration of C-17.

Furthermore, we obtained prugosene A1 from culture broth of another fungus *Penicillium* sp. FKI-5329, and measured the NFRD inhibitory activity.[11] The IC_{50} values of prugosene A1 against NFRD and NADH oxidase were 13 nM and 8600 nM, respectively, similar to those of **1**. The data suggested that the (17*S*)-epimer was more potent inhibitor and the conformation of dihydropyran ring was much more important than 2-oxabicyclo[2.2.1]heptane unit for *Ascaris* enzyme-specific inhibition. In addition, the results indicated the methyl moiety at C-8 did not affect the inhibitory activity.

We evaluated the cytotoxicity of **1** using human T-lymphocyte Jurkat cells by MTT method.[12] Morphological change and growth inhibition were observed by **1** at high concentration. The IC_{50} value of growth inhibition was 21 μM, about 8800 times weaker than that of NFRD inhibition (2.4 nM). Antimicrobial activities of **1** were tested by an agar dilution method.[13] As well as prugosenes,[8] **1** did not show antimicrobial activities against Gram-positive and Gram-negative bacteria and fungi at 100 μg/mL (214 μM). Therefore, **1** and prugosene A1 are expected to be selective and potent NFRD inhibitors.

4. Experimental

4.1. General

UV spectra were measured by Hitachi UV/Vis spectrometer U-2810. Optical rotations were recorded by means of JASCO DIP-1000 polarimeter. FT-IR spectra were conducted on Horiba FT-170. NMR spectra were recorded on 300 MHz (Varian XL-300), 400 MHz (Varian XL-400), and 600 MHz (Varian Inova 600) NMR spectrometer. For calibration of ^{13}C and ^{1}H chemical shifts, the carbon signal and residual proton signal of $CDCl_3$ were used ($CDCl_3$: δ_H 7.26 ppm and δ_C 77.0 ppm). FABMS and HRFABMS spectra were measured on JEOL JMS-AX505HA. Normal phase HPLC analysis was

performed using Pegasil silica column (4.6φ×250 mm) applying $CHCl_3$/acetone (100:1). Reverse phase HPLC analysis was performed using Pegasil ODS column (4.6φ×250 mm) applying CH_3CN/H_2O (65:35). Adults *A. suum* and bovine heart were purchased from Tokyo Shibaura Zouki Co. Ltd.

4.2. Organisms

The fungus *Penicillium* sp. FKI-3389 was isolated from a soil sample collected in Hilo, Hawaii, USA. By the sequence data of ITS rDNA and morphological characteristics, the fungus FKI-3389 was identified to be a member of the *Penicillium* genus. The ITS sequence of the strain FKI-3389 was deposited at the DNA Data Bank of Japan with accession number AB455515. The fungus FKI-3389 was deposited at the NITE Patent Microorganisms Depositary, National Institute of Technology and Evaluation, Kisarazu, Chiba, Japan as NITE BP-244.

4.3. Fermentation

One loopful of the strain FKI-3389 grown on LcA slant (glycerol 0.1%, KH_2PO_4 0.08%, K_2HPO_4 0.02%, $MgSO_4 \cdot 7H_2O$ 0.02%, KCl 0.02%, $NaNO_3$ 0.2%, and agar 1.5%, pH 6.0) was inoculated into 500-mL Erlenmeyer flask containing 100 mL of a seed culture medium (glucose 2%, yeast extract 0.2%, $MgSO_4 \cdot 7H_2O$ 0.05%, polypeptone 0.5%, KH_2PO_4 0.1%, and agar 0.1%, pH 6.0) and incubated on a rotary shaker at 27 °C for 2 days. A 1-mL of the seed culture was inoculated into each of sixty 500-mL Erlenmeyer flasks containing a production medium (50 g of water-sodden rice). Fermentation was carried out statically at 27 °C for 13 days.

4.4. Isolation

Moldy rice (3 kg) was extracted with 3.0 L of EtOAc. After the rice was removed by filtration the extract was concentrated in vacuo to afford a brown oil (14 g). The oil was applied to a silica gel column (48φ×450 mm) and washed with $CHCl_3$. Active materials eluted with $CHCl_3$/MeOH (100: 1) were concentrated to yield a crude material (2.7 g), which was then chromatographed over another silica gel column (30φ×330 mm). After washing with $CHCl_3$, the active materials were eluted with $CHCl_3$/MeOH (100:0 to 100:1). The active materials (1.9 g) were purified by preparative HPLC (column, Pegasil silica, 20φ×250 mm; mobile phase, $CHCl_3$/acetone (100:1); flow rate, 7.0 mL/min; detection, UV at 360 nm). Ukulactones A (**1**) and B (**2**) were eluted at 11 and 17.5 min, respectively. Each fraction was concentrated to dryness in vacuo to afford ukulactones A (**1**, 515 mg) and B (**2**, 3.5 mg) as yellow syrups.

*4.4.1. Ukulactone A (**1**).* Yellow syrup; $[\alpha]_D^{25}$ −54.0 (*c* 0.1, MeOH); UV (MeOH) λ_{max} (log ε) 243 (sh, 3.38), 308 (sh, 4.29), 325 (4.60), 340 (4.78), 358 (4.76) nm; IR ν_{max} (NaCl) 3730, 3595, 2927, 2858, 1795, 1745 cm^{-1}; HRFABMS *m/z* 466.2722 ($[M]^+$, 466.2719 calcd for $C_{29}H_{38}O_5$); ^1H and ^{13}C NMR, see Table 1.

*4.4.2. Ukulactone B (**2**).* Yellow syrup; $[\alpha]_D^{25}$ +87.5 (*c* 0.1, MeOH); UV (MeOH) λ_{max} (log ε) 245 (sh, 3.30), 309 (sh, 4.07), 325 (4.38), 340 (4.55), 359 (4.51) nm; IR ν_{max} (NaCl) 3730, 3593, 2922, 2856, 1797, 1743 cm^{-1}; HRFABMS *m/z* 466.2710 ($[M]^+$, 466.2719 calcd for $C_{29}H_{38}O_5$); ^1H and ^{13}C NMR, see Table 1.

4.5. Biological studies

4.5.1. Enzyme assays. NADH-fumarate reductase inhibitory activity was assayed using submitochondrial particles of *A. suum*. For the preparation of these particles containing NADH-fumarate reductase, muscle of *A. suum* (1 g) was homogenized in 3.5 mL of sodium phosphate buffer (120 mM, pH 7.0) and centrifuged at 1000×g for 10 min to remove cell debris. The supernatant was further centrifuged at 10,000×g for 30 min and the resultant mitochondrial precipitate was re-suspended in 3.5 mL of sodium phosphate buffer (120 mM, pH 7.0) before use.

NADH-fumarate reductase inhibitory activity was assayed by the following procedure; 80 μL of sodium phosphate buffer (120 mM, pH 7.0) containing 0.35 mM NADH and 7.2 mM disodium fumarate and 10 μL of DMSO/H_2O (1:1) solution of test compound were put into a 96-well plate and shaken for 3 min. The reaction was initiated by the addition of 10 μL of the submitochondrial fraction and the resultant mixture was incubated for 3 min at 37 °C. After incubation, absorbance at 340 nm was observed every 15 s for 10 min at 37 °C. The inhibitory activity was calculated as followed.

$$\text{Inhibition}(\%) = \left\{1 - \frac{\left(A_{slope}[\text{sample}] - A_{slope}[\text{no fumerate}]\right)}{\left(A_{slope}[\text{control}] - A_{slope}[\text{no fumerate}]\right)}\right\} \times 100$$

A: Absorbance at 340 nm.

NADH oxidase inhibitory activity and succinate-cytochrome *c* reductase inhibitory activity were assayed using submitochondrial particles of bovine heart. For preparation of submitochondrial particles from bovine heart muscles, chopped muscle (1 g) was homogenized in 5 mL of 120 mM sodium phosphate buffer (pH 7.0) and centrifuged at 1000×g for 10 min. The supernatant was further centrifuged at 10,000×g for 30 min and the resultant mitochondrial precipitate was re-suspended in 3.5 mL of sodium phosphate buffer (120 mM, pH 7.0). The suspension was centrifuged at 100,000×g for 30 min after ultrasonication and the submitochondrial particles were obtained as a precipitate. Before use, the precipitate was re-suspended in 3.5 mL of sodium phosphate buffer (120 mM, pH 7.0).

NADH oxidase inhibitory activity was assayed as follows: the phosphate buffer (80 μL) containing 0.70 mM NADH and 10 μL of DMSO/H_2O (1:1) solution of test compound were put into a 96-well plate and shaken for 3 min. The reaction was initiated by the addition of 10 μL of the submitochondrial fraction and the mixture was incubated for 3 min at 37 °C. After incubation, absorbance at 340 nm was observed every 15 s for 10 min at 37 °C. The inhibitory activity was calculated as followed.

$$\text{Inhibition}(\%) = \left\{1 - \frac{\left(A_{slope}[\text{sample}] - A_{slope}[\text{no enzyme}]\right)}{\left(A_{slope}[\text{control}] - A_{slope}[\text{no enzyme}]\right)}\right\} \times 100$$

A: Absorbance at 340 nm.

Succinate-cytochrome *c* reductase (SCRD) inhibitory activity was assayed by the following procedure: phosphate buffer (80 μL) containing 7.2 mM sodium succinate, 2.0 mg/mL of bovine cytochrome *c* and 1.3 mM potassium cyanide and 10 μL of DMSO/H_2O (1:1) solution of test compound were put into a 96-well plate and shaken for 3 min. The reaction was initiated by addition of 10 μL of the submitochondrial fraction and the mixture was incubated for 3 min at 37 °C. After incubation, absorbance at 550 nm was observed every 15 s for 10 min at 37 °C. The inhibitory activity was calculated as followed.

$$\text{Inhibition}(\%) = \left\{1 - \frac{\left(A_{slope}[\text{sample}] - A_{slope}[\text{no succinate}]\right)}{\left(A_{slope}[\text{control}] - A_{slope}[\text{no succinate}]\right)}\right\} \times 100$$

A: Absorbance at 550 nm.

Other enzyme activities were measured as described previously.[2a,14]